Strategy With Smooth Transitions and Improved Torque–Speed Region and Stator Copper Loss for Two-Level Asymmetrical Six-Phase Induction Motor Drives Under Switch Faults

Alejandro G. Yepes, *Senior Member, IEEE*, Jesús Doval-Gandoy, *Member, IEEE*, and Hamid A. Toliyat, *Fellow, IEEE*

***Abstract*—Asymmetrical six-phase drives are very attractive to obtain fault tolerance. Most faults arise in the power electronics. Two conventional methods to handle switch/diode faults in two-level converters are keeping the corresponding phases open (in two-level multiphase drives) or connecting them to the dc-link midpoint (in two-level three-phase drives) through a bidirectional switch (e.g., triac/relay). However, the former yields larger stator copper loss (SCL) for given torque and smaller maximum torque, because of current constraints; on the other hand, the latter reduces the maximum speed, due to voltage constraints, and has not been considered for two-level multiphase drives. This article presents several proposals to improve fault-tolerant behavior in two-level asymmetrical six-phase induction motor drives. First, to adequately combine and alternate said two approaches in these particular drives, depending on the speed, neutral-point configuration, and faulty legs. In this manner, the SCL-per-torque decreases and the total torque–speed region of the drive is extended, i.e., the maximum torque and maximum speed rise compared with each of the aforementioned conventional strategies. Second, to also turn ON/OFF a switch between stator neutral points for further improvement in this regard. Third, a pulsewidth modulation procedure to ensure smooth transitions between drive configurations. Experimental results confirm the theory.**

***Index Terms*—Fault tolerance, fault tolerant control, multiphase drives, six-phase drives, variable speed drives.**

Nomenclature

Acronyms

1CDF α_1–β_1 current derating factor, i.e., derating factor [1] or maximum α_1–β_1 current modulus (normalized).
1N Single neutral point.
2 N Two (isolated) neutral points.
FRMLS Full-range minimum-loss strategy.
IGBT Insulated-gate bipolar transistor.
IPMSM Interior PMSM.
PMSM Permanent-magnet synchronous machine.
PWM Pulsewidth modulation.
SCL Stator copper loss.
SN Configuration with bidirectional switch between neutral points.

Subscripts and superscripts

op Open phase.
opt Optimum for dc-link utilization, i.e., as in (12).
prev Previous.
rc Rated (and healthy) conditions.
zs Zero sequence.

I. Introduction

Multiphase drives (i.e., with more than three phases) offer important benefits in comparison with three-phase ones, including better fault tolerance [2], [3]. In particular, six-phase motors with asymmetrical winding arrangement are the most popular type of multiphase machine [1]–[19].

In an electric drive, the faults due to the power electronics are the most frequent [3], [20]. The faults in the usual converter switches or their freewheeling diodes [henceforth, simply referred to as insulated-gate bipolar transistors (IGBTs)] can be classified into open- and short-circuit ones [3], [21].

The postfault behavior of an electric drive depends on the converter topology and its number of levels. Although multilevel converters such as T-type three-level ones [17]–[19] permit higher efficiency and voltage than two-level converters, the latter are commonplace in multiphase drives [2], [22], [23] and, thus, of significant relevance. Some of the reasons for the popularity of the latter are that for two levels the voltage synthesis is less complex and that fewer semiconductors and firing signals are needed.

In fault-tolerant drives, when a fault occurs a dedicated algorithm should detect it and diagnose its nature properly as soon

Manuscript received April 7, 2020; revised June 8, 2020; accepted July 21, 2020. Date of publication July 24, 2020; date of current version September 22, 2020. This work was supported in part by the Ministry of Science, Innovation and Universities under the Ramon y Cajal Grant RYC2018-024407-I, and in part by the Spanish Ministry of Science and Innovation, and in part by the European Commission, European Regional Development Fund (ERDF) under Project PID2019-105612. Recommended for publication by Associate Editor Z. Zhang. *(Corresponding author: Jesús Doval-Gandoy.)*

Alejandro G. Yepes and Jesús Doval-Gandoy are with the Applied Power Electronics Technology (APET) Research Group, University of Vigo, Vigo 36310, Spain (e-mail: agyepes@uvigo.es; jdoval@uvigo.es).

Hamid A. Toliyat is with the Department of Electrical and Computer Engineering, Texas A&M University, College Station, TX 77843 USA (e-mail: toliyat@tamu.edu).

Color versions of one or more of the figures in this article are available online at https://ieeexplore.ieee.org.

Digital Object Identifier 10.1109/TPEL.2020.3011852

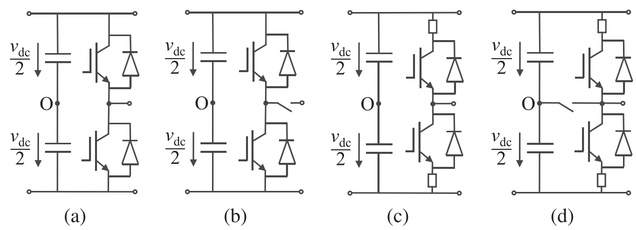

Fig. 1. Schematic of two-level converter dc-link and an arbitrary leg. (a) Without extra elements. (b) With an additional switch per line. (c) With a fuse per IGBT. (d) With a bidirectional switch (e.g., a triac or relay) to connect to O and a fuse per IGBT; this is used for the proposal in this article.

as possible [3], [24]. This subject has been in itself the focus of extensive research, including methods specifically targeted at asymmetrical six-phase drives [15], [16], [19]. Subsequently, a fault-tolerant strategy, suitable for the particular type of fault identified, should be adopted [3], [24].

In the literature, the tolerance to IGBT faults is normally addressed differently in two-level drives with three phases and in those with more phases.

On the one hand, in two-level multiphase drives (with star connection), it is usually considered that after an IGBT fault occurs the current through such phase is zero, either for open-circuit [1], [3]–[9], [16], [25]–[29] or short-circuit ones [1], [3], [9], [16], [27]. In the latter case, an additional switch (e.g., circuit breaker, relay, etc.) in the line [see Fig. 1(b)] [1], [9], [24], [27] or a fuse in series with an IGBT [see Fig 1(c)] [24] is opened, so that the system behaves as for an open-circuit fault. Compared with healthy conditions, having the faulty phase[1] open results in substantial reduction of the maximum torque [or equivalently, derating factor[2] [1], i.e., α_1–β_1 current derating factor (1CDF)] that can be achieved without exceeding the rated current, as well as an stator copper loss (SCL) increase (for given torque) [1], [3], [4], [6], [7], [26].

On the other hand, in two-level three-phase drives a common fault-tolerant procedure is to provide a current path through a bidirectional switch (e.g., a triac or relay) connected to the dc-link midpoint O [see Fig. 1(d)] [24], [30]–[32]. If the IGBT fault is of short-circuit type, turning ON this bidirectional switch blows a fuse in series with the faulty IGBT [24], [32]. Then, the terminal[3] voltage of such phase is fixed to the voltage of O, the corresponding phase current is given by the other phase currents, and the 1CDF and SCL-per-torque become as good as if the faulty leg were healthy. However, the maximum speed without overmodulation is then reduced to roughly half the rated speed ω^{rc} [30], [32]. This is because the maximum acceptable value of the line-to-line voltage (nearly proportional to speed ω) should then be imposed, in the worst-case scenario, between a dc-link positive/negative pole and its midpoint O, rather than between the two poles. In addition, to prevent overcurrent, it is not recommendable to connect (fix) several phases to O if there is a current path through a common stator neutral point. Accordingly, in three-phase machines this method is limited to just one leg. To the knowledge of the authors, fixing one or more phases to O has not been considered for two-level multiphase drives so far.

In sum, if one or more IGBTs are faulty in a two-level drive, traditionally the postfault performance is worsened in one of the following ways until it is repaired, without any switching between these modes.

1) The 1CDF is reduced and the SCL-per-torque increases, if the phase is kept in open circuit (normally applied in two-level multiphase drives [1], [3]–[9], [16], [25]–[29]).
2) The maximum speed is decreased, if a phase is connected to O (often applied in three-phase drives, to just one phase [24], [30]–[32]).

The possibility of adequately combining and alternating these two modes in a single two-level drive has not been considered so far. Two-level multiphase machines, with their capability to continue working under one or more open phases, offer the potential to conveniently combine and alternate these modes to attain a superior postfault performance, but it has not been studied before and it is not straightforward. Furthermore, in multiphase drives there are various neutral-point configurations [1], [4], [9], [12]; hence, it may also be possible to further improve the postfault performance by alternating the neutral-point configurations in a suitable combination with the switching between the aforesaid two operation modes of the inverter legs. Although it has been proposed to change online the neutral configuration (near ω^{rc}) in a two-level six-phase drive [9], only open phases (without fixing to O) were taken into account. Considering simultaneously, the connection/disconnection of phases to O, and of the star neutral points to each other, reinforces the nontrivial character of bringing together these conventional approaches that have never been studied in conjunction. Moreover, special care should be devoted to design the pulsewidth modulation (PWM) method so that it does not cause undesired currents flowing through the bidirectional switches and the corresponding stator phases, especially at the instant of turning them ON.

It is worth mentioning that the possibility of having one or two phases fixed to O continuously was considered in [17]–[19] as a result of certain fault scenarios in asymmetrical six-phase drives based on T-type three-level inverters. However, the topology and its behavior differs from two-level ones, only the case of isolated stator neutral points (i.e., 2 *N*) was studied, and no alternation between drive configurations was applied during postfault operation to further enhance the performance. In particular, as a consequence of the abovementioned limitation, when adopting these strategies the maximum speed (for faults such that a phase is fixed to O) or the 1CDF and SCL-per-torque (for faults such that a phase is open) are expected to be worse than they could be if drive reconfiguration were applied.

In this article, a fault-tolerant strategy is presented for two-level asymmetrical six-phase induction motor drives under one

[1]Through this article, the expression "faulty phase" (or similar) is also used to refer to the cases where it is not the stator phase itself what is faulty, but the IGBTs of the respective leg (the latter is the focus of this article).

[2]The derating factor or 1CDF is the maximum torque/flux-producing (α_1–β_1) current modulus, normalized by rated (and healthy) conditions, δ, that can be obtained in a certain fault scenario without any phase current surpassing its rating [1]. The maximum achievable torque increases with the 1CDF [1].

[3]The term "terminal" makes reference to a stator phase ending (typically, opposite to the neutral point) that is available on the outside of the machine for connecting to other external wires [3], [5], [25].

TABLE I
SUMMARY OF MAIN DIFFERENCES BETWEEN THIS ARTICLE AND THE STATE-OF-THE-ART

Postfault strategy	Phase number	Converter levels	Machine type	Alternation of drive configurations during postfault operation for better performance	PWM for smooth transitions	Main drawback compared with this paper
Connect to O a phase with IGBT faults [24], [30]–[32]	3	2	Various	No	No	$\omega \leq \omega^{\mathrm{rc}}/2$
Direct-torque control, space-vector PWM and current/voltage compensation [17]–[19]	6	3	PMSM	No	No	$\omega \leq \omega^{\mathrm{rc}}/2$ or worse 1CDF and SCL-per-torque
Minimum-loss, maximum-torque or FRMLS (faulty legs kept open) [1], [3]–[8], [25]–[29]	5-15	2	Induction /PMSM	No	No	Worse 1CDF and SCL-per-torque
FRMLS considering field-weakening (faulty legs kept open) [9]	6	2	IPMSM	1N/2N at ω^{rc}	No	Worse 1CDF and SCL-per-torque and abrupt transitions
This paper	6	2	Induction	Open/fixed-to-O phases and 1N/2N at $\omega^{\mathrm{rc}}/2$	Yes (carrier-based)	–

or more open- or short-circuit IGBT faults. Namely, this strategy consists of the following three novel proposals.

1) In the first place, it is proposed to connect some faulty phases to O (depending on the neutral configuration and faulty IGBTs) when the speed is below $\omega^{\mathrm{rc}}/2$, and to open such phases when it is higher. A twofold enhancement is attained with respect to conventional strategies. On the one hand, the 1CDF is extended and the SCL-per-torque is decreased in comparison with the usual two-level multiphase approach of keeping all faulty phases open. On the other hand, the maximum speed is increased (and often the 1CDF and SCL are also better, by fixing to O several phases) when compared with the three-phase technique of fixing to O one phase.
2) It is also proposed to use a bidirectional switch between the two stator neutral points, adequately combining its switching with the aforementioned alternation between open/fixed phases. This permits to increase to a substantial extent the amount of enhancement in such terms.
3) Moreover, a novel carrier-based PWM procedure is proposed to avoid excessive current peaks during the transitions between these various drive configurations.

Experimental results of all these improvements are provided. In this manner, in agreement with the preceding discussion, the main differences between this article and the state of the art can be summarized, as shown in Table I. The preliminary version [13] just included simulation results, only steady state (not the transitions) was considered, and many fault scenarios were not addressed.

This article is organized as follows. Section II reviews some fundamentals about fault-tolerant asymmetrical six-phase induction motor drives. Then, in Section III, the proposed strategy is described in detail, focusing on the steady-state performance. The PWM is adapted in Section IV to ensure a smooth transition between drive configurations. The experimental results are presented in Section V. Finally, Section VI summarizes the conclusion.

II. BACKGROUND

A. Neutral-Point Configurations

The stator of an asymmetrical six-phase machine consists of two three-phase stars (winding sets), shifted by $\gamma = \pi/6$ (see

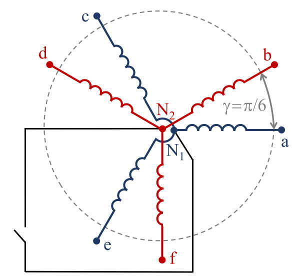

Fig. 2. Stator windings of an asymmetrical six-phase machine, for SN neutral-point configuration (a switch is used between the neutral points).

Fig. 2). The neutral points (N_1 and N_2) of the stars[4] can be connected (1N), isolated from each other (2 *N*), or sharing a bidirectional switch as in Fig. 2 (SN) [9]. For healthy drive, 2 *N* yields lower SCL than 1N [12]. Under open phases, 1N offers better SCL-per-torque and 1CDF than 2*N* [1].

B. Vector Space Decomposition

A stator electrical variable x (voltage v or current i) can be transformed from per-phase values to six orthogonal axes, which pairwise form the planes α_1–β_1, α_3–β_3, and α_5–β_5 [7]

$$[x_{\alpha_1}\ x_{\beta_1}\ x_{\alpha_3}\ x_{\beta_3}\ x_{\alpha_5}\ x_{\beta_5}]^{\mathrm{T}} = H\,[x_{\mathrm{a}}\ x_{\mathrm{b}}\ x_{\mathrm{c}}\ x_{\mathrm{d}}\ x_{\mathrm{e}}\ x_{\mathrm{f}}]^{\mathrm{T}} \quad (1)$$

$$H = \frac{1}{3}\begin{bmatrix} 1 & \cos(\gamma) & \cos(4\gamma) & \cos(5\gamma) & \cos(8\gamma) & \cos(9\gamma) \\ 0 & \sin(\gamma) & \sin(4\gamma) & \sin(5\gamma) & \sin(8\gamma) & \sin(9\gamma) \\ 1 & \cos(3\gamma) & \cos(12\gamma) & \cos(15\gamma) & \cos(24\gamma) & \cos(27\gamma) \\ 0 & \sin(3\gamma) & \sin(12\gamma) & \sin(15\gamma) & \sin(24\gamma) & \sin(27\gamma) \\ 1 & \cos(5\gamma) & \cos(20\gamma) & \cos(25\gamma) & \cos(40\gamma) & \cos(45\gamma) \\ 0 & \sin(5\gamma) & \sin(20\gamma) & \sin(25\gamma) & \sin(40\gamma) & \sin(45\gamma) \end{bmatrix}. \quad (2)$$

Assuming sinusoidally distributed windings, i_{α_1} and i_{β_1} are related to rotor flux and torque, whereas the other two plane currents, only to losses [2]. The α_3–β_3 (often called zero-sequence) current is restricted by $i_{\alpha_3} = -i_{\beta_3}$ and $i_{\alpha_3} = i_{\beta_3} = 0$ for 1N and 2 *N*, respectively [12], which according to (1) and (2) is

[4] Although for 1N it could be understood that there is a single six-phase star, henceforth, the term star refers to a three-phase winding set, even for 1N.

equivalent to

$$i_{\rm a}+i_{\rm b}+i_{\rm c}+i_{\rm d}+i_{\rm e}+i_{\rm f}=0 \qquad \text{for 1 N} \tag{3}$$

$$i_{\rm a}+i_{\rm c}+i_{\rm e}=0;\quad i_{\rm b}+i_{\rm d}+i_{\rm f}=0 \qquad \text{for 2 N.} \tag{4}$$

C. Relation of α_1–β_1 Current With Rotor Flux and Torque

In a frame with orthogonal axes d_1 and q_1 rotating in the α_1–β_1 plane, with the d_1 axis aligned with the rotor flux $\psi_{\rm r}$, typically $\psi_{\rm r}$ is set to its rated value by a constant i_{d_1}, and the torque is linearly adjusted with i_{q_1}, in both healthy [33] and faulty [4] drive. The α_1–β_1 current modulus

$$|i_{\alpha_1\beta_1}|=\sqrt{i_{\alpha_1}^2+i_{\beta_1}^2}=\sqrt{i_{d_1}^2+i_{q_1}^2} \tag{5}$$

can be normalized as

$$\delta=\frac{|i_{\alpha_1\beta_1}|}{|i_{\alpha_1\beta_1}^{\rm rc}|} \tag{6}$$

where rc means rated (healthy) conditions. Torque is proportional to δ^2 [1]. In healthy and steady state, $\delta\in[0\%,100\%]$.

D. Review of the Full-Range Minimum-Loss Strategy (FRMLS) for Obtaining 1CDF and SCL

The FRMLS, based on calculating the current references so as to minimize the SCL for each δ value (torque and flux) under the fault constraints, yields the largest 1CDF (maximum achievable δ) and lowest SCL-per-δ for certain fault and drive configuration [6], [7].

1) Review of the FRMLS: Since i_{α_1} and i_{β_1} set rotor flux and torque, currents references can be written as [1], [4], [6]

$$I=\begin{bmatrix}i_{\alpha_1} & i_{\beta_1} & i_{\alpha_3} & i_{\beta_3} & i_{\alpha_5} & i_{\beta_5}\end{bmatrix}^{\rm T}=H_k\begin{bmatrix}i_{\alpha_1} & i_{\beta_1}\end{bmatrix}^{\rm T} \tag{7}$$

$$H_k=\begin{bmatrix}1 & 0 & k_{\alpha_3,\alpha} & k_{\beta_3,\alpha} & k_{\alpha_5,\alpha} & k_{\beta_5,\alpha}\\ 0 & 1 & k_{\alpha_3,\beta} & k_{\beta_3,\beta} & k_{\alpha_5,\beta} & k_{\beta_5,\beta}\end{bmatrix}^{\rm T}. \tag{8}$$

The optimum H_k for each δ is obtained by minimizing the SCL (normalized by healthy and rated conditions) [6], [7]

$$J=\frac{I^{\rm T}I}{|i_{\alpha_1\beta_1}^{\rm rc}|^2}=\frac{\sum_{\sigma=1,3,5}\left(i_{\alpha_\sigma}^2+i_{\beta_\sigma}^2\right)}{(i_{\alpha_1}^{\rm rc})^2+(i_{\beta_1}^{\rm rc})^2}=\frac{I^{\rm T}I}{(i^{\rm rc})^2} \tag{9}$$

while satisfying for any α_1–β_1 phase angle [6], [7] the current constraints (3) and (4) and (op stands for open phase/s)

$$i_{\rm op}=0 \tag{10}$$

$$\max\{|i_\phi|\}/i^{\rm rc}\le 1,\ \phi={\rm a,b,c,d,e,f}. \tag{11}$$

The latter means that no phase current surpasses its rated value.

In this minimization problem, it is not necessary to include torque ripple (ideally zero, in absence of harmonics), mechanical loss (function of ω), core loss (depends only on i_{α_1} and i_{β_1}), or inverter loss (indirectly optimized with J) [7], [8].

The converter voltage constraints are ignored for the FRMLS as well because, assuming constant $i_{\rm d_1}$ [4], [33] and negligible stator-impedance voltage drop, they are only related to speed, not to current. Furthermore, using zero-sequence noncurrent-producing voltage for extra dc-link utilization [14], [34] reinforces the validity of disregarding stator-impedance voltage drop, because it diminishes the effect of its postfault unbalance on the dc-bus exploitation [26]. For more accuracy, current-dependent voltage constraints may be added [9]. However, this introduces motor-parameter dependence, and the associated ω extension [9] is small compared with that studied here (from $\omega^{\rm rc}/2$ to $\omega^{\rm rc}$) and it could simply be added afterward.

2) Obtaining the SCL-Per-δ and 1CDF: The normalized SCL for given δ equals J after solving for H_k the minimization problem (1)–(11) with cost function (9) [6], [7], [26]. The 1CDF for certain fault and drive configuration is the largest δ such that this problem has solution [6], [7], [26], i.e., such that no phase current (increasing with δ) exceeds its rating [see (11)] [1]. Since (1)–(11) do not depend on motor parameters and a whole cycle of α_1–β_1 current is considered in every problem iteration for given δ, the 1CDF and normalized SCL-per-δ are independent of motor parameters and i_{d_1}/i_{q_1} ratio [1], [26]. Thanks to the normalization by rated current in (6), (9), and (11), the 1CDF and SCL values (expressed as percentages of rated ones) do not vary with motor rating either [1], [26]. The highest achievable torque increases with the 1CDF [1], [26].

It should also be emphasized that the FRMLS is not a contribution of this article. The FRMLS has been presented and used in previous publications [6], [7], and it is here employed just as a tool to quantify the improvement in 1CDF and SCL attained by the method proposed here (next section), based on conveniently adapting the drive configuration. In [6] and [7], the drive configuration was not altered after fault; namely, faulty phases were always kept open, and only 1N was considered.

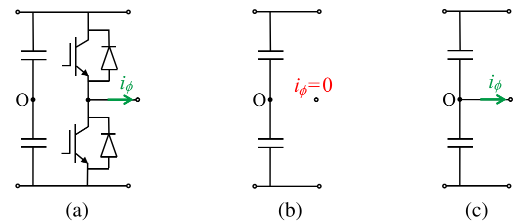

Fig. 3. Equivalent representation of an inverter leg of the type shown in Fig. 1(d) when using the proposed strategy and the leg is (a) healthy, (b) faulty and actively kept open, (c) faulty and actively fixed to O.

III. Proposed Method for Improvement of the Torque–Speed Region and SCL

Instead of keeping faulty phases open, as usual in two-level multiphase drives [1], [3]–[9], [16], [25]–[29], or fixed to O, as done (for just one phase) in two-level three-phase drives [24], [30]–[32], it is proposed in Sections III-A and III-B to adequately combine and alternate these strategies in two-level six-phase drives with 1N or 2 *N*, using Fig. 1(d) configuration for each leg. Under single or double IGBT faults per leg, Fig. 1(d) topology permits to either keep the phase open or fixed to O, as represented in Fig. 3. It is assumed that an algorithm (out of scope) detects and diagnoses the fault when it occurs, turns OFF the gating signals of both IGBTs in the leg, and if it is of short-circuit type, turns ON the bidirectional switch to blow the fuse in series [24], [32]. To stabilize the O voltage, it is advisable, e.g., to oversize

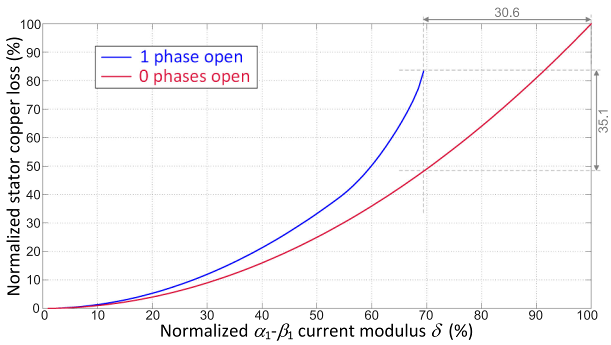

Fig. 4. SCL-versus-δ comparison, with 1N and an IGBT fault in one phase, depending on whether such phase is kept open (conventional two-level multiphase approach [6], [7]) or fixed to O (proposed).

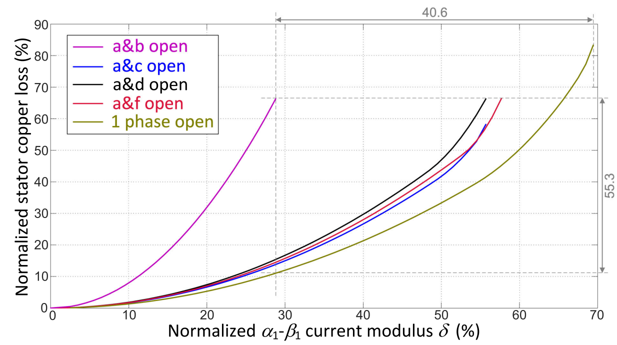

Fig. 5. SCL-versus-δ comparison, with 1N and IGBT faults in two phases, for various scenarios: phases a and b open, a and c open, a and d open, a and f open (conventional two-level multiphase approaches [7]), and lastly one phase open and one fixed to O (proposed).

the capacitors [24], [30] or to add balancing resistors [35]. In Section III-C, the possibility of conveniently using SN to further improve the performance is addressed in detail. Finally, in Section III-D, several general guidelines to implement the proposed strategy are summarized.

A. Improvement for 1N

Regardless of the number of faulty legs, for 1N with the proposed strategy at most only one phase should be fixed to O. Otherwise, overcurrent may arise in the loops involving the dc link and the stator neutral point.

If only one leg is faulty, the respective phase can be switched between open/fixed modes [Fig. 3(b) and (c)]. Fig. 4 shows the SCL-versus-δ curves, assessed with the FRMLS from Section II-D, assuming for generality that actual currents track their references perfectly. The differences between the different fault/configuration scenarios are related to the constraint (10), which determines in which phases current flow is allowed. Note that the blue curve in Fig. 4 corresponds to the conventional approach for two-level multiphase drives of keeping the faulty phase open [6], [7]. From Fig. 4, for any δ the SCL is reduced when fixing the phase to O. For instance, for $\delta = 69.4\%$, which is the 1CDF (maximum δ) for open phase,[5] the SCL decrease is 35.1%. Regarding the 1CDF, when fixing to O the 1CDF rises by 30.6%, from 69.4% to 100%.

When several legs are faulty, the SCL and 1CDF depend on which phases are affected [7]. Fig. 5 shows SCL-versus-δ for several scenarios of two faulty phases. All the curves except the beige one represent the conventional two-level multiphase approach [7] of keeping both faulty phases open. Due to machine symmetry, all possibilities of two open phases are implicitly considered. Table II illustrates which cases of two faulty phases are analogous due to symmetry [1], [7]. The beige curve in Fig. 5 illustrates the situation with one (any) of such faulty phases fixed to O, so that only one phase remains open. From this figure, the SCL and 1CDF improvement when the phase is fixed to O is

[5]Henceforth, when a phase is said to be open or in open circuit, it is meant that such phase is kept without current path. These expressions are not used to refer to a phase with open-circuit IGBT fault/s that has been afterward fixed to O, unless it is explicitly stressed.

TABLE II
EQUIVALENT TWO-OPEN-PHASE CASES DUE TO SPATIAL SYMMETRY

Spatial angle between open phases	Equivalent cases of open phases
$\pi/6$	a&b $\equiv$ c&d $\equiv$ e&f
$2\pi/3$	a&c $\equiv$ a&e $\equiv$ c&e
$5\pi/6$	a&d $\equiv$ c&f $\equiv$ b&e
$\pi/2$	a&f $\equiv$ b&c $\equiv$ d&e

substantial for any two faulty legs. In particular, for faults in phases a and d, the 1CDF rises by 40.6%, and the SCL (e.g., for the maximum δ for both phases open) is reduced by 55.3%. The SCL-versus-δ curves and 1CDF values are not a contribution of this article, but rather selecting the optimum configurations for each situation and adequately switching between them to provide the best performance at each moment. It should also be remarked that although, e.g., the beige curve in Fig. 5 can also be found in [6] in which this performance was achieved with single-phase fault, whereas here it is attained under two faulty phases thanks to the proposed strategy.

If the faulty legs are three or more, the choice of the phase to switch between open/fixed modes (the other two are kept open) is no longer irrelevant. The FRMLS can be used to assess the SCL-versus-δ curves for the scenarios that result by fixing each (one at a time) faulty phase to O. From the resulting plots, the phase to switch between modes can be chosen. For instance, for faults in phases a, c, and f, the behavior in various cases is compared in Fig. 6. Up to roughly $\delta = 54.6\%$, the lowest SCL-per-δ is obtained by fixing phase f to O (a and c open). For $\delta > 54.6\%$, it is preferable to fix phase c to O, so that the SCL-per-δ is the lowest and the 1CDF is the largest. In this manner, the 1CDF with respect to keeping the three phases open (conventional approach [1]) is increased by 16.9%, and the SCL (for, e.g., the maximum δ for the three phases open) is reduced by 11.1%. Less importantly, alternating between fixing to O phases c or f at $\delta \approx 54.6\%$ reduces the SCL-per-δ by up to approximately 2%, compared with fixing phase f to O regardless of δ. Since a 2% difference is small, in practice the latter may be preferred. It is worth noticing that, although the red and beige curves were given in [7], in that case such behavior was obtained

TABLE III
1CDF FOR DIFFERENT OPEN-PHASE SCENARIOS [1], [7]

Neutrals	No open phases	One (any) open	a&b open	a&c open	a&d open	a&f open	a&b&c open	a&c&d open	a&c&e open	a&c&f open
1N	100%	69.4%	28.8%	55.7%	55.7%	57.7%	12.2%	14.9%	50.0%	40.8%
2N	100%	57.7%	28.8%	50.0%	28.8%	57.7%	∅	∅	50.0%	∅

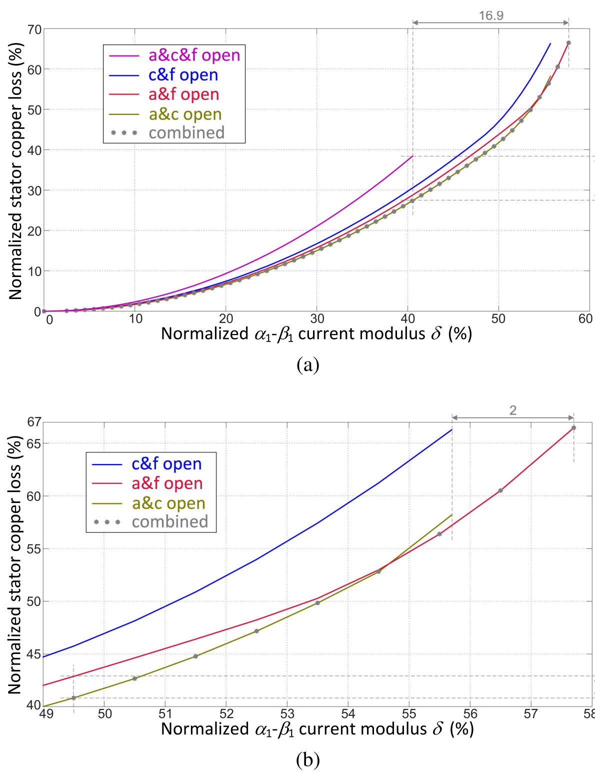

Fig. 6. SCL-versus-δ comparison, with 1N and IGBT faults in phases a, c, and f, for different scenarios: the three phases are kept open (conventional two-level multiphase approach), phase a is fixed to O, phase c is fixed to O, phase f is fixed to O, and the strategy combining the previous two cases (proposed approaches). (a) General view. (b) Zoom on the rightmost part.

under two faulty phases, whereas in this article it is achieved for three faulty phases.

To facilitate choosing the phases to fix to O in other open-phase situations, the 1CDF for all of them is shown in Table III, in accordance with the data in [1] and [7]. The ∅ symbol means unfeasible operation. The fault scenarios of more than two phases that are equivalent due to spatial symmetry can be easily found analogously to Table II. It can be checked that the 1CDFs in Table III for 1N match the maximum δ in Figs. 4–6 for the respective cases. Furthermore, indirectly the 1CDF values are also useful to select the best options in terms of SCL, because usually the SCL-per-δ is smaller when 1CDF is larger [6], [7]. For instance, from Table III, for 1N and faults in phases a, c, d, and f, it is convenient to fix phase d to O (1CDF $=$ 40.8%) instead of, e.g., phase f (1CDF $=$ 14.9%). Note that the 1CDF values in Table III were given in [1], [7] for the strategy based on keeping all faulty phases open, whereas in this article the same performance is obtained under a higher number of faulty phases, thanks to the proposal of fixing some to O.

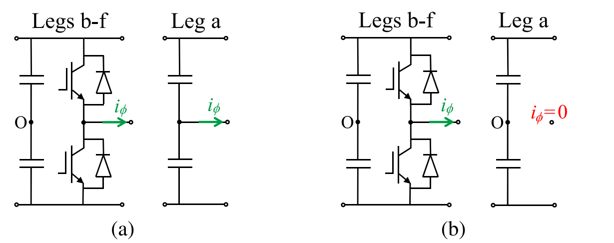

Fig. 7. Representation of proposed strategy for 1N with IGBT fault/s in phase a. (a) $\omega < \omega^{\rm rc}/2$. (b) $\omega > \omega^{\rm rc}/2$.

Fixing a phase to O halves the maximum voltage (or ω) that can be obtained in the inverter output without overmodulation. [30], [32]. Thus, for 1N, it is here proposed to fix a phase (chosen as aforesaid) to O when $\omega < \omega^{\rm rc}/2$, and to open it otherwise, as depicted in Fig. 7. A hysteresis band can be used at $\omega \approx \omega^{\rm rc}/2$.

Fig. 8(a) illustrates the torque–speed (δ versus $\omega/\omega^{\rm rc}$) region with 1N and faults in phases a and d, for three strategies: keeping both phases open (left), fixing to O one of them (center), and the proposal of combining both depending on ω (right). The two values (55.7% and 69.4%) of maximum δ (1CDF) in Fig. 8(a) mach those of the corresponding curves (black and beige) in Fig. 5 and the respective numbers in Table III. Most importantly, it can be observed in Fig. 8(a) that, by switching one phase between the open/fixed modes when $\omega \approx \omega^{\rm rc}/2$, the torque–speed area is extended (see the rightmost region, in beige). On the one hand, in comparison with keeping both phases open (usual in multiphase drives [1], [7]), the maximum δ (1CDF) rises from 55.7% to 69.4% for $\omega < \omega^{\rm rc}/2$. This 1CDF increase also comes with an SCL-per-δ reduction, in accord with the black and beige lines in Fig. 5. On the other hand, compared with keeping a phase fixed to O (as in some three-phase drives [24], [30]–[32]), the proposal increases the maximum ω from $\omega^{\rm rc}/2$ to $\omega^{\rm rc}$.

The 1CDF quantities that limit the areas in Fig. 8(a) at the top, and the associated SCL, would vary for other faulty legs. Nevertheless, the main conclusion from this figure, about the convenience of alternating both modes at $\omega \approx \omega^{\rm rc}/2$, can be applied to other 1N fault scenarios. The proposed configurations for 1N are summarized in Table IV, where ∅ indicates unfeasible operation. Fixing a phase to O at low speeds is desirable for faults in one, two or three phases, whichever they are. For faults in four phases, the drive would also be able to work for $\omega < \omega^{\rm rc}/2$ by fixing one phase to O, but not for $\omega > \omega^{\rm rc}/2$. With more than four faulty legs, the motor cannot run even at low speed, because of the fault severity. Table V shows the improvement achieved in this manner for 1N and $\omega < \omega^{\rm rc}/2$ in each fault situation, with respect to the conventional two-level six-phase strategy of keeping faulty phases open [1], [6], [7]. It is expressed in

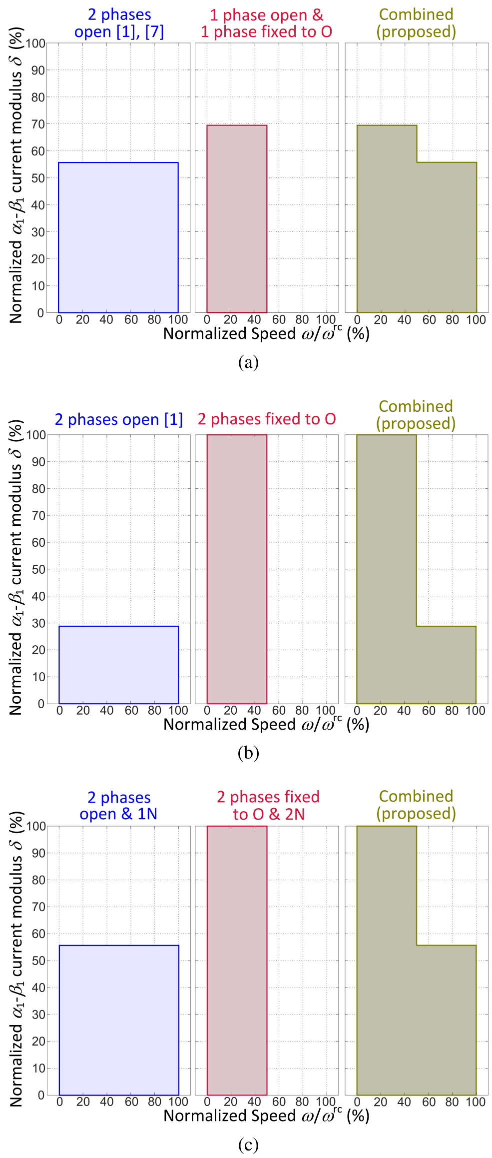

Fig. 8. Comparison of δ-speed region with faults in phases a and d, for several fault-tolerance approaches: both phases kept open (left), one (any) or both of them fixed to O (center), and the proposal based on alternating the mode of one phase depending on the speed (right). (a) 1N. (b) 2 *N*. (c) SN.

TABLE IV
PROPOSED CONFIGURATIONS FOR 1N

Phases with faulty IGBTs	Phases fixed to O	
	$\omega < \omega^{rc}/2$	$\omega > \omega^{rc}/2$
0	0	0
Between 1 and 3	1	0
4	1	∅
> 4	∅	∅

terms of SCL (at the 1CDF of the conventional method) and in terms of 1CDF. These values match those given through this section for particular examples, such as in Figs. 4–6 and 8(a). From Table V, in every scenario with a number of faulty legs between one and three, the proposal yields smaller SCL and greater 1CDF, as expected. For four faulty legs, although the conventional strategy is not able to run the machine at all, with the novel method it becomes possible for $\omega > \omega^{rc}/2$.

TABLE V
FOR 1N, IMPROVEMENT FOR $\omega < \omega^{rc}/2$ OVER CONVENTIONAL STRATEGY FOR TWO-LEVEL SIX-PHASE DRIVES (KEEPING FAULTY PHASES OPEN WITH 1N [1], [6], [7])

Phases with faulty IGBTs	Open phases for proposed configuration	1CDF increase (%)	SCL reduction (%) (at convent. 1CDF)
None	None	100 → 100	100 → 100
One (any)	None	69.4 → 100	83.3 → 48.2
a&b	One (any)	28.8 → 69.4	66.3 → 11.1
a&c	One (any)	55.7 → 69.4	58.2 → 41.5
a&d	One (any)	55.7 → 69.4	66.3 → 41.5
a&f	One (any)	57.7 → 69.4	66.5 → 45.2
a&b&c	b&c	12.2 → 57.7	29.3 → 2.6
a&b&d	a&c	14.9 → 55.7	31.1 → 4.3
a&c&e	Two (any)	50.0 → 55.7	50.0 → 41.7
a&c&f	a&f	40.8 → 57.7	38.4 → 29.1
a&b&c&d	a&c&d	∅ → 14.9	–
a&b&c&e	a&c&e	∅ → 50.0	–
a&b&c&f	a&c&f	∅ → 40.8	–
a&b&d&e	a&d&e	∅ → 40.8	–
More than 4	∅	∅ → ∅	∅

– Not possible to compute the SCL improvement at the 1CDF of the conventional strategy, because the latter does not exist in such case.

TABLE VI
PROPOSED CONFIGURATIONS FOR 2N

Phases with faulty IGBTs			Phases fixed to O			
			$\omega < \omega^{rc}/2$		$\omega > \omega^{rc}/2$	
Total	Winding $k = 1$	Winding $k = 2$	Winding $k = 1$	Winding $k = 2$	Winding $k = 1$	Winding $k = 2$
0	0	0	0	0	0	0
1	1	0	1	0	0	0
2	1	1	1*	1*	0	0
2	2	0	1	0	0	0
3	2	1	1	1	0	0
3	3	0	0	0	0	0
4	2	2	1	1	∅	∅
4	3	1	0	1	∅	∅
> 4	Any	Any	∅	∅	∅	∅

* Exception: if the faulty phases are $\pi/2$ apart spatially, identical performance is obtained without fixing any to O; thus, it is not needed.

B. Improvement for 2 N

For 2N and $\omega < \omega^{rc}/2$ two phases can be fixed to O without overcurrent, if they are not of the same star. Otherwise, only one of them can be fixed to O, as for 1N. When $\omega > \omega^{rc}/2$, due to voltage constraints none can be fixed to O, as for 1N as well. Accordingly, the configurations in Table VI are proposed for the scenarios with 2N. Due to symmetry, $k = 1$ and $k = 2$ can be swapped in the table, as long as it is done in all its columns. Whenever there is one or two phases with faults in the same three-phase winding set k, one of them is fixed to O for $\omega < \omega^{rc}/2$, regardless of the other star. An exception to this statement (as indicated in Table VI) is when there are two faulty phases and they are $\pi/2$ apart spatially (e.g., a and f), since then the performance with one phase open would be exactly the same (compare the cases of one phase and of a&f open in the

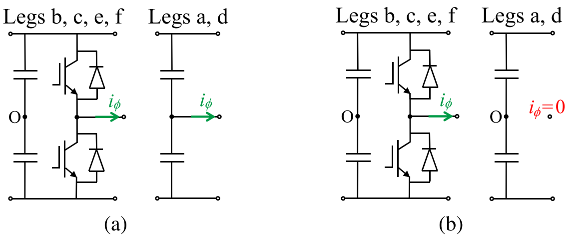

Fig. 9. Representation of proposed strategy for 2 N with IGBT faults in phases a and d. (a) $\omega < \omega^{\rm rc}/2$. (b) $\omega > \omega^{\rm rc}/2$.

TABLE VII
FOR 2N, IMPROVEMENT FOR $\omega < \omega^{\rm rc}/2$ OVER CONVENTIONAL STRATEGY FOR TWO-LEVEL SIX-PHASE DRIVES (KEEPING FAULTY PHASES OPEN WITH 2N [1])

Phases with faulty IGBTs	Open phases for proposed configuration	1CDF increase (%)	SCL reduction (%) (at convent. 1CDF)
None	None	$100 \to 100$	$100 \to 100$
One (any)	None	$57.7 \to 100$	$66.5 \to 33.3$
a&b	One (any)	$28.8 \to 57.7$	$66.3 \to 14.5$
a&c	One (any)	$50.0 \to 57.7$	$50.0 \to 43.8$
a&d	One (any)	$28.8 \to 57.7$	$66.3 \to 14.5$
a&f	a&f	$57.7 \to 57.7$	$66.5 \to 66.5$
a&b&c	b&c	$\varnothing \to 57.7$	–
a&b&d	a&c	$\varnothing \to 55.7$	–
a&c&e	a&c&e	$50.0 \to 50.0$	$50.0 \to 50.0$
a&c&f	a&f	$\varnothing \to 57.7$	–
a&b&c&e	a&c&e	$\varnothing \to 50.0$	–
Other	$\varnothing$	$\varnothing \to \varnothing$	$\varnothing$

– Not possible to compute the SCL improvement at the 1CDF of the conventional strategy, because the latter does not exist in such case.

last row of Table III). Similarly, in agreement with Tables III and VI, if the three phases of a star are faulty, fixing one to O does not make any difference. In addition, from Table VI, as for 1N (cf. Table IV) when there are four faulty legs operation is only possible if $\omega < \omega^{\rm rc}/2$, and when there are more, the drive cannot work at any ω.

For example, with faults in phases a and d, for $\omega < \omega^{\rm rc}/2$. [see Table VI and Fig. 9(a)]. Thus, the 1CDF rises from 28.8% (open phases) to 100% [see Fig. 8(b)]. It is also obvious, comparing the red curve in Fig. 4 with the black one in Fig. 5, that the SCL-per-δ is greatly reduced. Additionally, by switching as proposed between modes at $\omega \approx \omega^{\rm rc}/2$ [see Table VI and Fig. 9(b)], the maximum speed is extended from $\omega^{\rm rc}/2$ (phases fixed to O) to $\omega^{\rm rc}$ in the rightmost region of Fig. 8(b).

The enhancement shown in Fig. 8(b) for the proposal in torque–speed region and SCL-per-δ can be achieved for other 2N fault scenarios (with the few aforesaid exceptions), with just quantitative differences in the amount of improvement. As reflected in Table VII, the proposed strategy (applying Table VI) yields a considerable improvement in 1CDF and SCL when compared with the conventional two-level six-phase strategy (faulty phases open) for 2 N [1] in most situations; only for three fault cases (rows) of the table the performance is unaltered.

TABLE VIII
PROPOSED CONFIGURATIONS FOR SN

Phases with faulty IGBTs			$\omega < \omega^{\rm rc}/2$		$\omega > \omega^{\rm rc}/2$	
Total	Winding $k=1$	Winding $k=2$	Neutrals	Phases fixed to O	Neutrals	Phases fixed to O
0	0	0	2N	0	2N	0
1	1	0	2N	1	1N	0
2	1	1	2N	2	1N	0
2	2	0	1N	1	1N	0
3	2	1	2N*	2*	1N*	0
3	3	0	1N	1	1N	0
4	2	2	2N	2	$\varnothing$	$\varnothing$
4	3	1	1N/2N	1	$\varnothing$	$\varnothing$
> 4	Any	Any	$\varnothing$	$\varnothing$	$\varnothing$	$\varnothing$

*Exception: if two of the faulty phases are $\pi/2$ apart spatially, for $\omega < \omega^{\rm rc}/2$ identical performance results by fixing just one (the other phase), with either 1N/2N; for $\omega < \omega^{\rm rc}/2$, in such case the choice 1N/2N is also irrelevant ideally. Nevertheless, due to practical zero-sequence current, 2N is better.

C. Improvement for SN

For SN, switching between 1N and 2N can be combined at $\omega \approx \omega^{\rm rc}/2$ with the aforesaid connection/disconnection of phases to O, to further improve postfault behavior. The configurations proposed for SN are displayed in Table VIII. They are derived by comparing for each scenario the 1CDF (see Table III) of the choices in Tables IV and VI. In this manner, optimal SCL-per-δ and highest 1CDF result in every situation.

As shown in Table VIII, under fault 1N is normally preferred over 2N when $\omega > \omega^{\rm rc}/2$. This is due to two facts. a) As aforementioned earlier, for high speeds all phases with faults should be open for both 1N and 2N. b) Ideally, for 1N, the 1CDF and SCL-per-δ are better (or at worst, equal) than for 2N with the same open phases (see a column of Table III) [1], [7]. The only fault case where 1N is not preferred over 2N for $\omega > \omega^{\rm rc}/2$ is for three-phase faults such that two of the affected phases are $\pi/2$ apart spatially (e.g., a and f). This is because, as mentioned in the note under Table VIII, in such condition ideally there is no difference in performance between 1N and 2N (57.7% 1CDF in Table III), but 2N is preferred to avoid nonideal zero-sequence current.

When $\omega < \omega^{\rm rc}/2$, 2 N is usually chosen (see Table VIII) because the associated capability to fix two phases to O, one in each star, normally yields better 1CDF (see Table III) and SCL-per-δ. There are a few cases where performance is maximized without exploiting this possibility of 2N, as for the first two rows of Table VIII, or for the fifth row in the exceptional situation that two of the three faulty phases are $\pi/2$ apart spatially (then, maximum performance results by fixing just one phase, i.e., the other one, with either 1N/2N). In these scenarios, 2N is also preferred because, although no α_3–β_3 current is needed in them either for 1N or 2N, the latter prevents undesired current between neutrals. There are also some scenarios where 1N should be set rather than 2N even at low speed. If there are two faulty legs, both involving the same three-phase star (fourth row of Table VIII), with either 1N or 2N only one phase can be fixed to O, which implies that with both configurations the same phases are open; the extra current degree of freedom of 1N then yields higher performance (see Table III). When three legs are faulty, and

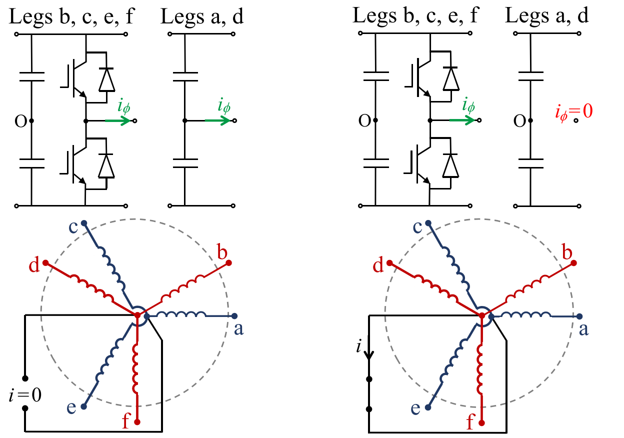

(a) (b)

Fig. 10. Representation of proposed strategy for SN with IGBT faults in phases a and d. (a) $\omega < \omega^{\mathrm{rc}}/2$. (b) $\omega > \omega^{\mathrm{rc}}/2$.

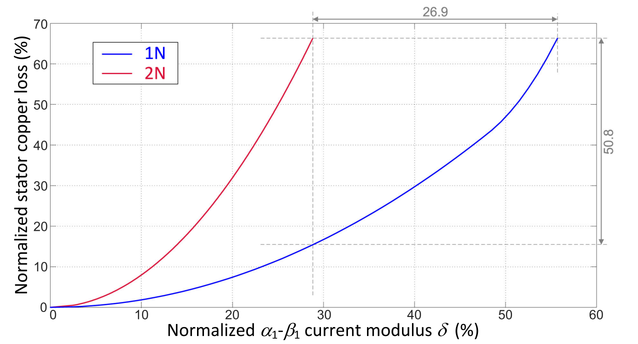

Fig. 11. SCL-versus-δ comparison, with phases a and d open, for 1 N or 2 N.

they all belong to a three-phase star (sixth row of Table VIII), both 1N and 2N exhibit equivalent behavior for $\omega < \omega^{\mathrm{rc}}/2$, but 1N becomes more suitable because, since for $\omega > \omega^{\mathrm{rc}}/2$ 1N is better, the bidirectional switch between neutrals would not have to be turned ON/OFFat $\omega \approx \omega^{\mathrm{rc}}/2$. Finally, if three phases of one star and one phase of the other star are affected by faults, then at low speed there is no preference between 1N and 2N, as indicated in the penultimate row of Table VIII. The reason is that no current flows between neutrals in either case and the performance is equivalent, provided that the open phase sharing a star with two healthy phases is fixed to O.

Let us consider again faults in phases a and d. As shown in the third row of Table VIII, at high ω the optimum is 1N with two open phases, and at low ω it is 2N with both fixed to O. These choices are illustrated in Fig. 10. The δ–ω regions for these individual configurations (ignoring the alternation between them) are depicted in the left and center parts of Fig. 8(c), respectively. They match the corresponding ones in Fig. 8(a) and (b). The area that results by applying the proposed strategy from Table VIII of combining these modes is shown in the right part of Fig. 8(c). The δ–ω region is extended not only compared with the other cases in Fig. 8(c), but also with those in the rightmost part of Fig. 8(a) and (b). For $\omega < \omega^{\mathrm{rc}}/2$, when comparing the complete proposal [right part of Fig. 8(c)] with the conventional two-level multiphase procedure using 1N [1], [7] [left part of Fig. 8(a)], the 1CDF is enhanced from 55.7% to 100% and the SCL-per-δ (e.g., at the 1CDF of the latter approach) from 66.3% to 31.0%, respectively (see Table III and compare the red curve in Fig. 4 with the black one in Fig. 5). Moreover, Fig. 11 shows that the amount of improvement obtained at high speed by changing from 2N to 1N as proposed (instead of keeping 2N, as for low ω) is 26.9% in 1CDF (in accord with Table III) and up to 50.8% in SCL-per-δ.

Table IX displays the enhancement provided by the complete proposal using SN, compared with the conventional two-level multiphase strategy (keeping faulty phases open with 1N) [1], [6], [7], for all fault scenarios. It can be observed that the

TABLE IX
IMPROVEMENT FOR $\omega < \omega^{\mathrm{rc}}/2$ USING SN OVER CONVENTIONAL STRATEGY FOR TWO-LEVEL SIX-PHASE DRIVES (KEEPING FAULTY PHASES OPEN WITH 1N [1], [6], [7])

Phases with faulty IGBTs	Proposed configuration Open phases	1N/2N	1CDF increase (%)	SCL reduction (%) (at convent. 1CDF)
None	None	1N	100 → 100	100 → 100
One (any)	None	1N	69.4 → 100	83.3 → 48.2
a&b	None	2N	28.8 → 100	66.3 → 8.3
a&c	a or c	1N	55.7 → 69.4	58.2 → 41.5
a&d	None	2N	55.7 → 100	66.3 → 31.0
a&f	None	2N	57.7 → 100	66.5 → 33.3
a&b&c	b&c	2N	12.2 → 57.7	29.3 → 2.6
a&b&d	b or d	2N	14.9 → 57.7	31.1 → 3.9
a&c&e	Two (any)	1N	50.0 → 55.7	50.0 → 41.7
a&c&f	a&f	2N	40.8 → 57.7	38.4 → 29.1
a&b&c&d	b&c	2N	∅ → 57.7	–
a&b&c&e	a&c&e	1N/2N	∅ → 50.0	–
a&b&c&f	a&f	2N	∅ → 57.7	–
a&b&d&e	d&e	2N	∅ → 57.7	–
More than 4	∅	∅	∅ → ∅	∅

– Not possible to compute the SCL improvement at the 1CDF of the conventional strategy, because the latter does not exist in such case.

configurations used in each situation with the proposal (second and third columns) are in agreement with those recommended in Table VIII. In all fault cases, the proposed technique achieves a considerably better performance, i.e., much higher 1CDF and lower SCL. For instance, for IGBT faults in phases a and b, it permits to raise the 1CDF from 28.8% to 100%, and to reduce the SCL at the conventional 1CDF from 66.3% to 8.3%. For faults in four phases, the proposal permits to run the drive (unlike the previous two-level six-phase methods), and with 1CDF of 50% or higher. The only fault conditions for which the performance is not enhanced are those with five or six phases affected by faults, because of the extreme severity.

D. General Principles to Apply the Proposed Method

In summary, in agreement with Tables IV, VI, and VIII, the proposed strategy can be implemented in general as follows.

For 1N (see Table IV), one faulty phase (the optimum) is fixed to O when $\omega < \omega^{\mathrm{rc}}/2$; and when $\omega > \omega^{\mathrm{rc}}/2$, it is opened.

For 2N (see Table VI), one faulty phase (the optimum) is fixed to O per star when $\omega < \omega^{\mathrm{rc}}/2$ (unless the three phases of such

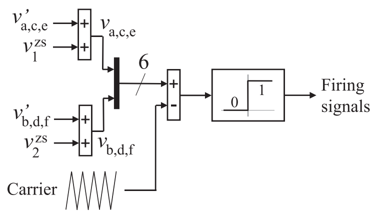

Fig. 12. General scheme of six-phase carrier-based PWM.

star are faulty, or if only two stator phases are faulty and they are spatially orthogonal); and when $\omega > \omega^{\mathrm{rc}}/2$, it is opened.

For SN (see Table VIII), which is preferred, the 2N approach is applied when $\omega < \omega^{\mathrm{rc}}/2$ (unless there are several faulty legs in a star and none in the other); and when $\omega > \omega^{\mathrm{rc}}/2$, 1N is set (except for healthy drive) and all faulty phases are opened. On the other hand, if a total of three stator phases are faulty and two of them are spatially orthogonal, instead, 2N is set for the whole speed range and when $\omega < \omega^{\mathrm{rc}}/2$ only the faulty phase that is not orthogonal is fixed to O.

IV. PWM Technique for Smooth Transitions

To avoid excessive current peaks, the voltage drop across the switches should be roughly zero before turning them ON. The PWM method proposed for this purpose is described in the following.

Fig. 12 depicts the PWM scheme. Carrier-based PWM is considered rather than space-vector PWM because, although there is always certain equivalence between both techniques, the former is simpler to implement [36]. In Fig. 12, when the PWM output for one healthy leg is high (1) or low (0), its top or bottom IGBT is turned ON, respectively. A zero sequence v_1^{zs} is added to the control output signals of the first star $v'_{\mathrm{a,c,e}}$, and a zero sequence v_2^{zs} is added to those of the second star $v'_{\mathrm{b,d,f}}$, yielding the modulating signals $v_{\mathrm{a,c,e}}$ and $v_{\mathrm{b,d,f}}$. The modulating signals of faulty phases are ignored. Accordingly, for convenience, here the concept of "zero sequence" is used to refer to the common mode of the healthy phases of a stator winding set. When not changing the drive configuration, to improve dc-link utilization, the zero-sequence voltages v_1^{zs} and v_2^{zs} may be set as [14], [34], [37]

$$v_k^{\mathrm{zs}} = v_k^{\mathrm{zs,opt}} = -0.5\left(\max\{v'_\phi\} + \min\{v'_\phi\}\right) \tag{12}$$

where ϕ sweeps through the healthy phases of the corresponding star k (both stars $k = 1, 2$, for 1 *N*). Equation (12) should not be applied if a phase is fixed to O in the same winding set (in any set, for 1 *N*), since then the zero-sequence current is used by the control to adjust the current of such phase.

First, a transition [see Fig. 8(c) and the third row of Table VIII] from 1 *N* with phases c and f open (equivalent to a and d; cf. Table II) to 2 *N* with phases c and f fixed to O is considered. Three bidirectional switches are turned ON/OFFin consecutive steps. The process is divided into the four situations (rows) in Table X. The voltage between the phase-ϕ (healthy or faulty) stator terminal and O is

TABLE X
PWM for Transition From 1N With c&f Open to 2N With c&f Fixed to O (or Vice Versa)

Situation	v_1^{zs}	v_2^{zs}
1N with c&f open	$v_1^{\mathrm{zs,prev}} + v_{1,2}^{\mathrm{zs,opt}}$	$v_2^{\mathrm{zs,prev}} + v_{1,2}^{\mathrm{zs,opt}}$
2N with c&f open	$-(3\dot{\psi}_{\mathrm{c}} + v'_{\mathrm{a}} + v'_{\mathrm{e}})/2$	$-(\dot{\psi}_{\mathrm{f}} + v'_{\mathrm{b}} + v'_{\mathrm{d}})/2 - \dot{\psi}_{\mathrm{c}}$
2N with c fixed, f open	$v_1^{\mathrm{zs,prev}}$	$-(3\dot{\psi}_{\mathrm{f}} + v'_{\mathrm{b}} + v'_{\mathrm{d}})/2$
2N with c&f fixed	$v_1^{\mathrm{zs,prev}}$	$v_2^{\mathrm{zs,prev}}$

$$v_{\phi\mathrm{O}} = R_{\mathrm{s}} i_\phi + \dot{\psi}_\phi + v_{N_k\mathrm{O}} \tag{13}$$

where R_{s} is the stator resistance, $\dot{\psi}_\phi$ is the time derivative of the stator flux linkage in phase ϕ, and $v_{N_k\mathrm{O}}$ is the voltage between the neutral N_k (k is 1 or 2, depending on ϕ) and O.

For 2N with phase c fixed to O and phase f open, v_{fO} should be set to to zero, so that phase f can be fixed to O without overcurrent. It is achieved by setting v_2^{zs} as shown in the respective cell of Table X. The v_2^{zs} term $-1/2(v'_{\mathrm{b}} + v'_{\mathrm{d}})$ cancels the $v'_{\mathrm{b}} + v'_{\mathrm{d}}$ value[6] that may exist before adding v_2^{zs}. The $1/2$ factor is included because v_2^{zs} is added to both v'_{b} and v'_{d}. On the other hand, $-3\dot{\psi}_{\mathrm{f}}$ is the $v_{\mathrm{b}} + v_{\mathrm{d}}$ value needed to yield $v_{\mathrm{fO}} = 0$. This is derived by checking that (13) gives $v_{N_2\mathrm{O}} = -\dot{\psi}_{\mathrm{f}}$ for $\phi = \mathrm{f}$ and $v_{\mathrm{fO}} = i_{\mathrm{f}} = 0$, while the sum of (13) for $\phi =$b, d, f results in $v_{\mathrm{bO}} + v_{\mathrm{dO}} = 3v_{N_2\mathrm{O}}$, assuming $\dot{\psi}_{\mathrm{b}} + \dot{\psi}_{\mathrm{d}} + \dot{\psi}_{\mathrm{f}} = 0$. The quantity $\dot{\psi}_{\mathrm{f}}$ can be obtained by applying the inverse transform H^{-1} to the stator flux linkage, estimated from the stator current and the steady-state motor model [33].

Analogously, the v_1^{zs} and v_2^{zs} formulas in Table X for 2N with two open phases provide $v_{N_1O} = v_{N_2O}$ and $v_{\mathrm{cO}} = 0$. Thus, the bidirectional switch between neutrals or between O and phase c can be closed without overcurrent.

The other v_1^{zs} and v_2^{zs} expressions in the table avoid the v'_ϕ terms, because in such conditions the $v'_{\mathrm{a}} + v'_{\mathrm{e}}$ and $v'_{\mathrm{b}} + v'_{\mathrm{d}}$ values are instead used for controlling the current between neutrals (for 1 *N*) or of phases fixed to O (last two rows), and hence, otherwise the dynamics could be worsened. To ensure this avoidance of v'_ϕ terms in v_1^{zs} and v_2^{zs}, while preventing abrupt transient disturbances in the new current paths being closed, the fundamental components in the individual signals v_1^{zs} and v_2^{zs} are maintained (oscillating) after such current paths are generated. For this purpose, v_k^{zs} passes through a bandpass filter (based, e.g., on negative feedback of integrators rotating at fundamental frequency) when no bidirectional switches connect star k to O or to the other star, and when the latter happens the filter bandwidth is set to zero, so that the filter output $v_k^{\mathrm{zs,prev}}$ no longer depends on any v'_ϕ terms. Then, $v_k^{\mathrm{zs,prev}}$ can be used for PWM, as shown in Table X. In addition, for 1 *N* with two open phases (see Table X), the optimum global zero-sequence $v_{1,2}^{\mathrm{zs,opt}}$

[6]For the situation of phase f open with 2N, such value of the current-control output can be removed/altered without any effect on the stator currents.

TABLE XI
PWM FOR TRANSITION FROM 1N WITH a OPEN TO 2N WITH a FIXED TO O (OR VICE VERSA)

Situation	v_1^{zs}	v_2^{zs}
1N with a open	$v_1^{\mathrm{zs,prev}} + v_{1,2}^{\mathrm{zs,opt}}$	$v_2^{\mathrm{zs,prev}} + v_{1,2}^{\mathrm{zs,opt}}$
2N with a open	$-(3\dot{\psi}_{\mathrm{a}} + v'_{\mathrm{c}} + v'_{\mathrm{e}})/2$	$-(v'_{\mathrm{b}} + v'_{\mathrm{d}} + v'_{\mathrm{f}})/3 - \dot{\psi}_{\mathrm{a}}$
2N with a fixed to O	$v_1^{\mathrm{zs,prev}}$	$v_2^{\mathrm{zs,prev}}$

TABLE XII
PWM FOR TRANSITION FROM 1 N WITH a&c OPEN TO 1 N WITH a FIXED TO O AND c OPEN (OR VICE VERSA)

Situation	v_1^{zs} + v_2^{zs}
1N with a&c open	$-(v'_{\mathrm{b}} + v'_{\mathrm{d}} + v'_{\mathrm{e}} + v'_{\mathrm{f}})/4 - \dot{\psi}_{\mathrm{c}}$
1N with a fixed to O, c open	$v_1^{\mathrm{zs,prev}} + v_2^{\mathrm{zs,prev}}$

TABLE XIII
PWM FOR TRANSITION FROM 1 N WITH a&c&d OPEN TO 2 N WITH a&d FIXED TO O AND c OPEN (OR VICE VERSA)

Situation	v_1^{zs}	v_2^{zs}
1N with a&c&d open	$v_1^{\mathrm{zs,prev}} + v_{1,2}^{\mathrm{zs,opt}}$	$v_2^{\mathrm{zs,prev}} + v_{1,2}^{\mathrm{zs,opt}}$
2N with a&c&d open	$-v'_{\mathrm{e}} - 2\dot{\psi}_{\mathrm{a}} - \dot{\psi}_{\mathrm{c}}$	$-(\dot{\psi}_{\mathrm{d}} + v'_{\mathrm{b}} + v'_{\mathrm{f}})/2 - \dot{\psi}_{\mathrm{a}}$
2N with a fixed, c&d open	$v_1^{\mathrm{zs,prev}}$	$-(3\dot{\psi}_{\mathrm{d}} + v'_{\mathrm{b}} + v'_{\mathrm{f}})/2$
2N with a&d fixed, c open	$v_1^{\mathrm{zs,prev}}$	$v_2^{\mathrm{zs,prev}}$

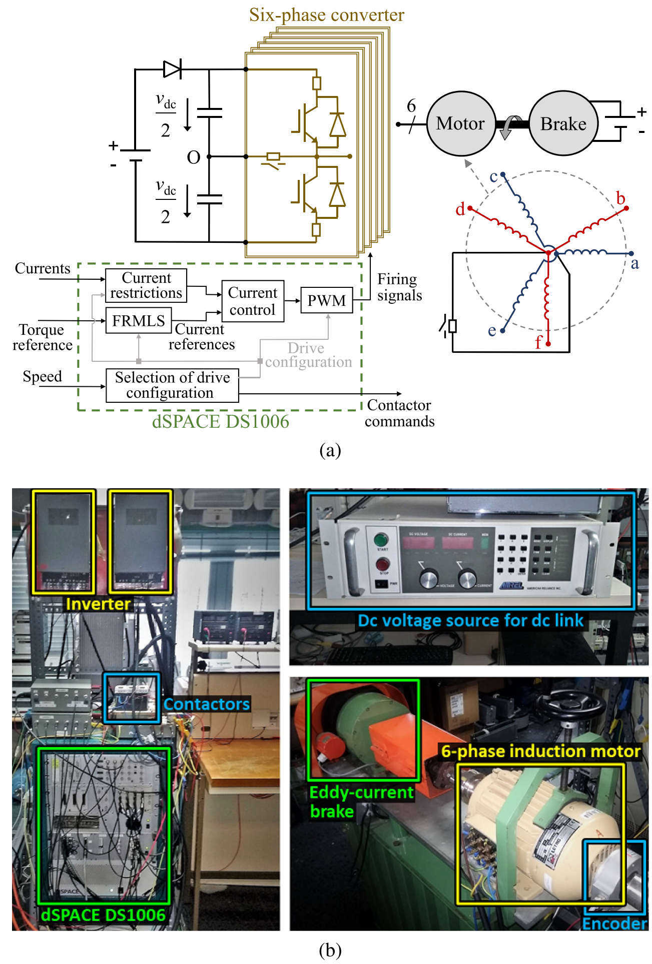

Fig. 13. Experimental setup. (a) Scheme. (b) Photographs.

from (12) can be added for better dc-link utilization, without affecting the currents.

The v_1^{zs} and v_2^{zs} expressions for other transitions can be obtained in a similar manner. Namely, Tables XI– XIII show those necessary for the second, fourth, and fifth rows of Table VIII, respectively. The third row of Table VIII has been addressed in Table X, and the other rows in Table VIII do not involve any transition related to the bidirectional switches. Regarding the exceptional case of the note under Table VIII, it can simply be performed analogously to the last two rows of Table XIII.

The current references should also be altered with the drive configuration, in accordance with the FRMLS. Furthermore, constraints (3) and (4) can be imposed to the measured currents.

V. EXPERIMENTAL RESULTS

A. Experimental Setup

The experimental setup is shown in Fig. 13. The six-phase motor is coupled to an eddy-current brake. Concerning the six-phase IGBT-based inverter, it is composed of two three-phase ones, the switching frequency is 10 kHz, and dead time is 3 μs. The total dc-link capacitance is 4 mF, and its voltage is kept at $v_{\mathrm{dc}} = 600$ V by a voltage source. The motor has one pole pair, stator, and rotor resistance of $R_{\mathrm{s}} = 6.7$ and 7 Ω, respectively, fundamental magnetizing inductance of 582 mH, α_1–β_1 stator and rotor leakage inductance of 38.2 and 12.8 mH, respectively, and α_5–β_5 stator leakage inductance of 5.2 mH. These parameters were estimated according to [11]. Rated speed and rated peak current of $\omega^{\mathrm{rc}} = 2540\ \mathrm{r/min}$ and $i^{\mathrm{rc}} = 2.7$ A are considered. In rated and healthy conditions, for field-oriented control the α_1–β_1 rated current modulus $|i_{\alpha_1\beta_1}| = 2.7$ A is distributed between the d_1 and q_1 axes as $i_{d_1} = 0.65$ A and $i_{q_1} = 2.62$ A, i.e., the rated rotor flux linkage and rated torque are $\psi_{\mathrm{r}}^{\mathrm{rc}} = 606\ \mathrm{mWb}$ and $4.7\ \mathrm{N \cdot m}$. The control is run at 10 kHz in dSPACE DS1006. Switching harmonics are removed by oversampling the measured currents at 10 MHz and averaging [7], [12]. Resonant controllers are implemented in the α_1–β_1 and α_5–β_5 planes at the fundamental [12], [28] and at low odd-order harmonic frequencies (to cancel undesired harmonics) [10], [12]. The control gains are tuned as in [12]. In the PWM scheme of Fig. 12, v_1^{zs} and v_2^{zs} are set according to (12) in the specified situations. Contactors with average impedance of 2.5 mΩ at 50 Hz are used as bidirectional switches to alter the drive configuration.

TABLE XIV
AVERAGE TORQUE AND i_{q_1} ($i_{d_1} = 0.65$ A) FOR EACH δ TESTED

δ (%)	28.8	55.7	69.4	100
i_{q_1} (A)	0.43	1.36	1.76	2.62
Torque (Nm)	0.77	2.43	3.15	4.70
Torque (%)	16.3	51.8	67.1	100

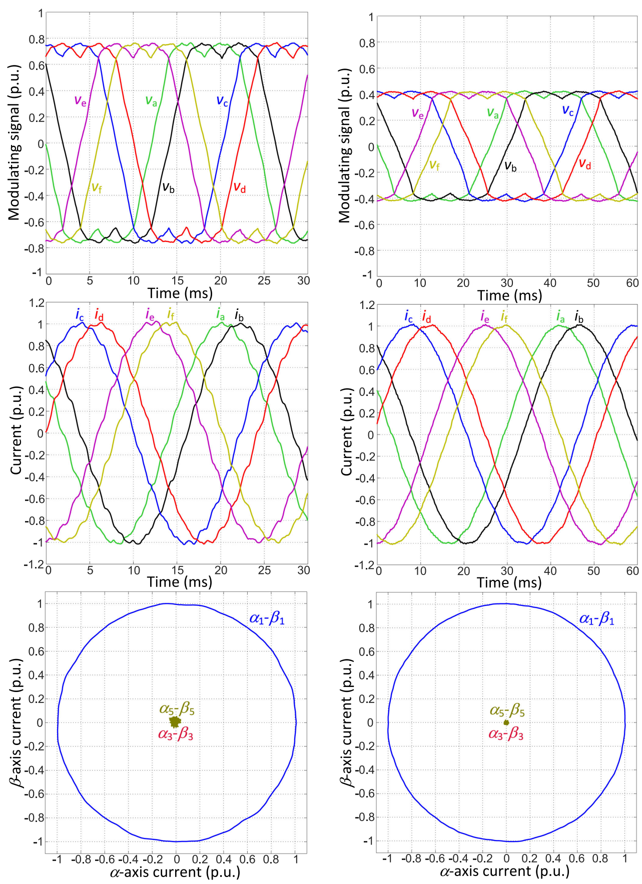

Fig. 14. Results for healthy drive, with 2 N, and at the healthy maximum δ (100%). (a) 2300 $\mathrm{r/min}$ (over $\omega^{\mathrm{rc}}/2$). (b) 1000 $\mathrm{r/min}$ (below $\omega^{\mathrm{rc}}/2$).

Table XIV displays the δ values being tested, as well as the respective average i_{q_1} and output torque, with the latter expressed in N·m and as a percentage of the rated torque.

B. Steady-State Results With Healthy Drive

First, the healthy behavior with 2 N is shown in Fig. 14. The motor is run at 2300 $\mathrm{r/min}$ and 1000 $\mathrm{r/min}$ with the rated peak current (1 p.u.). It can be checked that δ is as expected 100%, the phase-current amplitudes are on the 1-p.u. boundary, and the output voltages (normalized by $v_{\mathrm{dc}}/2$) are within the available margin. The modulating signals are relatively close to their limit at 2300 $\mathrm{r/min}$, but very far from it at 1000 $\mathrm{r/min}$. The phase currents and their plane trajectories are similar for both speeds, just with different frequency. The currents and voltages are practically balanced. At higher speed the current harmonics are canceled to a lower extent, because their frequencies tend to spread in the spectrum, and hence, be less affected by the control proportional gain. The most noticeable current harmonic is a principal rotor slot harmonic, which could be used for speed estimation [7].

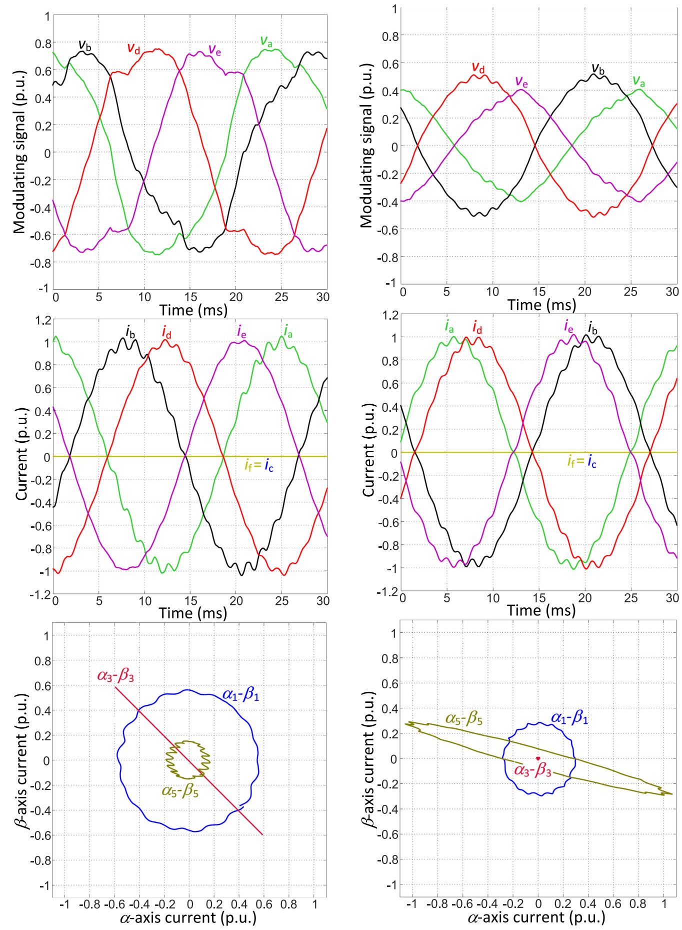

Fig. 15. Results for phases c and f open, at 2300 $\mathrm{r/min}$ (over $\omega^{\mathrm{rc}}/2$), and at the maximum δ for each case. (a) 1 N ($\delta = 55.7\%$). (b) 2 N ($\delta = 28.8\%$).

C. Steady-State Results With IGBT Faults in Phases c and f

In the following, faults are considered in phases c and f, which is equivalent to faults in phases a and d (see Table II). This scenario is chosen (as in Fig. 8) because it is a representative one, involving three bidirectional switches. If the results confirm the theory for this case, it can be stated that they also indirectly verify it to a great extent for other (mostly less general) scenarios, since the theoretical approach was essentially the same for all of them.

Fig. 15 shows results at 2300 $\mathrm{r/min}$ for 1N [see Fig. 15(a)] and 2N [see Fig. 15(b)], each at the respective 1CDF (55.7% and 28.8%). Since $\omega > \omega^{\mathrm{rc}}/2$, no phases are fixed to O. The currents of all healthy phases reach the maximum value of 1 p.u., in accordance with the fact that it is the maximum δ for each scenario. 1N allows much larger α_1–β_1 current than 2N, i.e., much greater 1CDF, as expected from theory. The slight

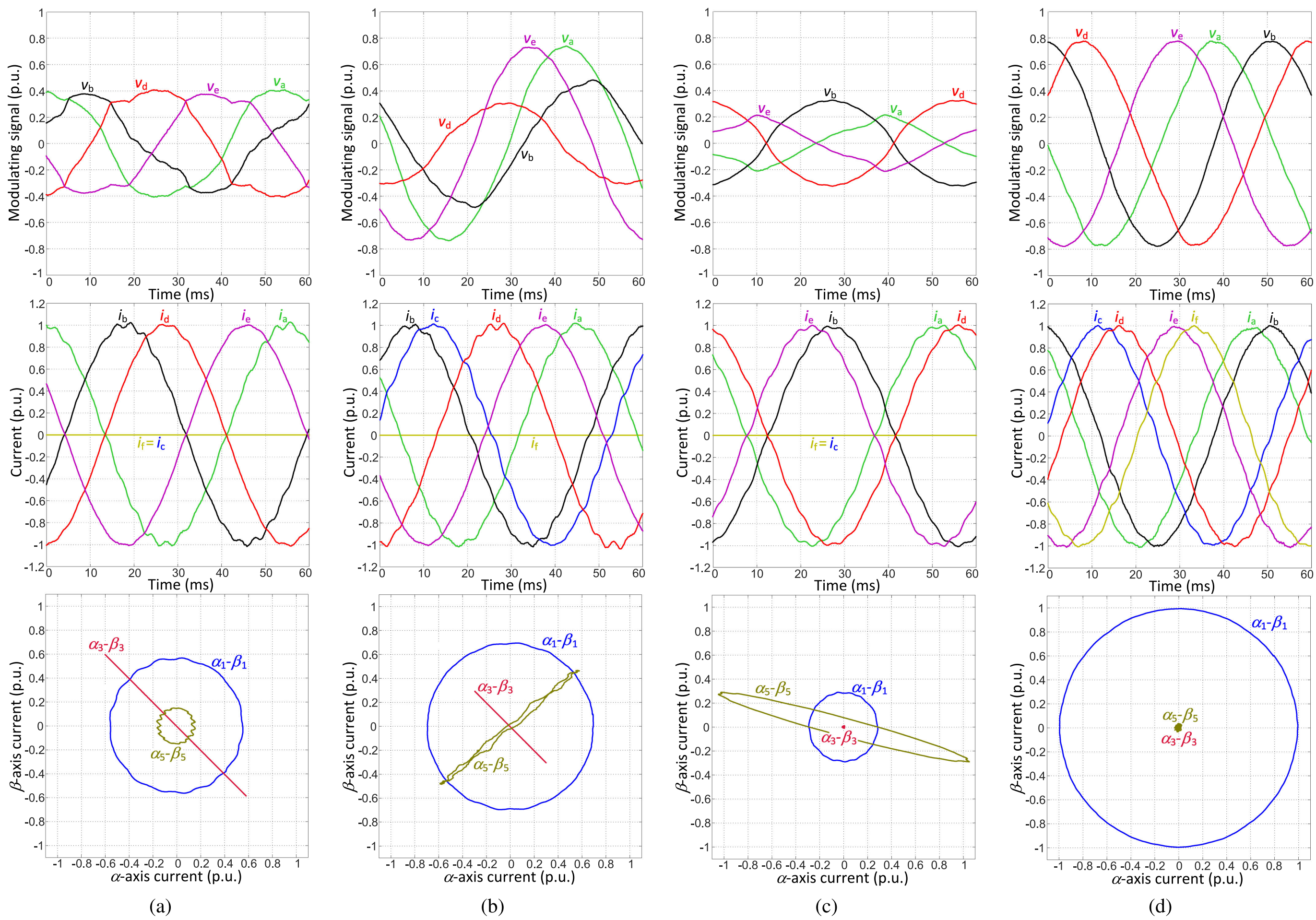

Fig. 16. Results for faults in phases c and f, at 1000 r/min (below $\omega^{\rm rc}/2$), and at the maximum δ for each case. (a) 1 N with both phases open ($\delta = 55.7\%$), i.e., conventional approach so far considered optimum for two-level six-phase drives [1], [7]. (b) 1 N with phase c fixed to O and phase d open ($\delta = 69.4\%$). (c) 2 N with both phases open ($\delta = 28.8\%$), as in [1]. (d) 2 N with both phases fixed to O ($\delta = 100\%$), i.e., the proposed strategy using SN (preferred).

difference among voltage amplitudes, in each case, is due to the unbalanced voltage drop (since the stator current is also unbalanced) across the stator impedance [5], [26], the latter of which is relatively large in this motor.

The current for $1000\ \mathrm{r/min}$ (below $\omega^{\rm rc}/2$) is shown in Fig. 16. In agreement with Fig. 8, there are two approaches for each neutral configuration. Fig. 16(a) and (b) shows the results for both phases open (conventional approach [1], [7]) and for phase c fixed to O, respectively, both with 1N. Concerning 2N, Fig. 16(c) and (d) shows the plots for both phases open and for both fixed to O, respectively. For each scenario in Fig. 16, the load torque is set so that δ is equal to the corresponding 1CDF (from left to right, 55.7%, 69.4%, 28.8%, and 100%). Indeed, since it is the maximum δ, the peak phase currents reach $1\ \mathrm{p.u.}$, except in the phases where constraints (3), (4), (10), and (11) prevent it. As expected, when the phases are fixed to O, current is allowed to flow, providing a greater modulus of α_1–β_1 trajectory, i.e., larger 1CDF. In this manner, the radius of the α_1–β_1 circumference is longer in Fig. 16(b) than in Fig. 16(a), and in Fig. 16(d) than in Fig. 16(c). The highest 1CDF is achieved for the proposed configuration with 2N and both phases fixed to O [see Fig. 16(d)], as expected from theory. It can also be

TABLE XV
SCL in the Experiments for IGBT Faults in Phases c and f

Speed (r/min)	δ (%)	1N & 2 open phases[†]	1N & 1 fixed phase	2N & 2 open phases	2N & 2 fixed phases
2500	28.8	14.9%*	∅	62.4%	∅
2500	55.7	66.2%*	∅	∅	∅
1000	28.8	15.4%	11.0%	61.2%	8.3%*
1000	55.7	66.1%	41.0%	∅	31.2%*
1000	69.4	∅	83.9%	∅	48.1%*
1000	100	∅	∅	∅	99.6%*

* Proposed strategy using SN (preferred).
† Conventional postfault strategy, so far considered optimum for two-level six-phase drives [7].

seen that when some phase is fixed to O [see Fig. 16(b) and (d)], the amplitude of the modulating signals is roughly doubled with respect to when it is not [cf. Fig. 16(a) and (c)]. This is in accord with the indication that such approach should only be applied for $\omega < \omega^{\rm rc}/2$.

Table XV displays the SCL for the δ and ω values tested in Figs. 14–16, but taking into account all possible drive configurations for each δ–ω pair. The normalized SCL is obtained as

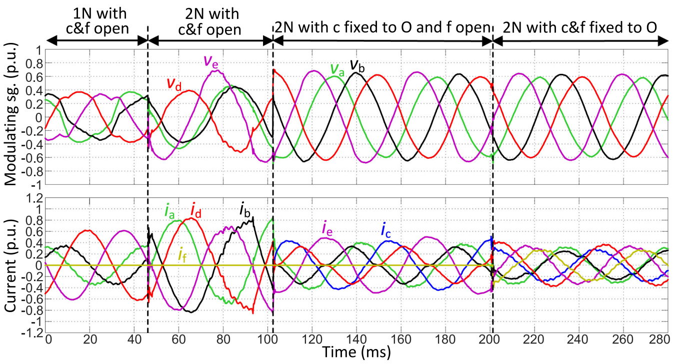

Fig. 17. With faults in phases c and f, results for transient between 1N with both phases open and 2N with both phases fixed to O, using proposed PWM.

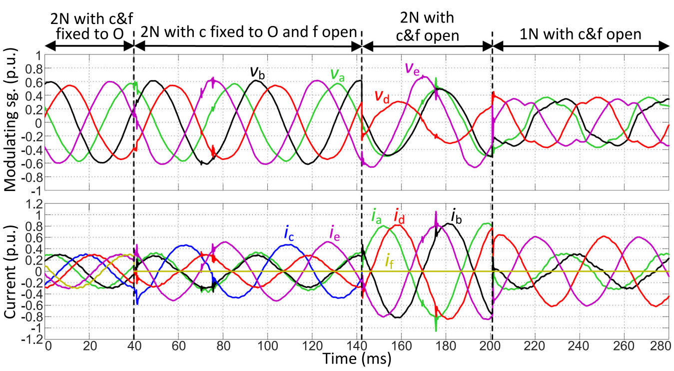

Fig. 18. With faults in phases c and f, results for transient between 2 N with both phases fixed to O and 1 N with both phases open (i.e., opposite to Fig. 17), using proposed PWM.

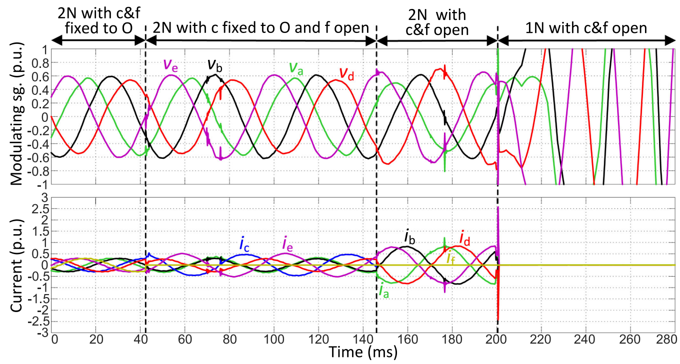

Fig. 19. With faults in phases c and f, results for transient between 2 N with both phases fixed to O and 1 N with both phases open, using conventional PWM.

$2\sum(i_\phi^{\mathrm{rms}})^2/(i^{\mathrm{rc}})^2$, where i_ϕ^{rms} is the rms for each phase current. Switching harmonics are disregarded. From Table XV, for given δ and ω, the lowest SCL-per-δ at high speed is provided by 1N, and the smallest SCL-per-δ at low speed is always attained by 2N with two phases fixed to O, as expected. As aforesaid, these options also match those that yield the largest 1CDF. It is, thus, convenient to install SN, so that 2N and 1N can be set at low and high speed, respectively, as proposed. The table also shows that the proposal (* cells) yields lower SCL-per-δ (less than half) and larger operation range (maximum δ increased from 55.7% to 100%) for $\omega < \omega^{\mathrm{rc}}/2$ than the conventional solution of 1N and two open phases, so far considered optimum [1], [7] for two-level asymmetrical six-phase drives, especially using FRMLS [7] († column). All these outcomes match the theory.

D. Transition Between Drive Configurations

Fig. 17 shows the results for the transition between 1N with phases c and f open and 2N with both phases fixed to O. The procedure proposed in Section IV is implemented. The speed is $1270\ \mathrm{r/min}$ $(\omega^{\mathrm{rc}}/2)$ and δ is set to 29%. The opposite transition is shown in Fig. 18. From Figs. 17 and 18, there are no substantial current peaks despite the switching of the contactors, thanks to the proposed PWM adaptation. In contrast, when these transients are tested with $v_1^{\mathrm{zs}} = v_2^{\mathrm{zs}} = 0$ in the PWM (see Fig. 12) there is overcurrent and the protections are triggered, interrupting the drive operation. For instance, this happens in Fig. 19 when the bidirectional switch between neutrals is closed. The moderate steady-state dissimilarities in the voltage and current waveforms among the four situations in Figs. 17 and 18 are due to the modifications in the PWM zero sequence and to the different FRMLS H_k coefficients in each of them. Note that the FRMLS behavior [6] is the reason why the current amplitudes are clearly unequal for the two situations with open phase/s and $1\mathrm{CDF} > \delta$.

If triacs or solid-state relays are used instead of electromechanical contactors, the transition time can be much shorter and less variable, at the cost of increased loss and complexity.

TABLE XVI
SUMMARY OF EXPERIMENTAL IMPROVEMENT OVER CONVENTIONAL TWO-LEVEL SIX-PHASE STRATEGY [7]

1CDF increase (%)	SCL reduction (%) (at $\delta = 55.7\%$)	Improvement in transitions
55.7 → 100	66.1 → 31.2	overcurrent→smooth

E. Summary of Experimental Improvement Over Conventional Two-Level Six-Phase Strategy [7]

Table XVI summarizes the experimental improvement provided by the proposed strategy in comparison with the conventional one for two-level asymmetrical six-phase drives based on keeping all faulty phases open with 1N [7]. The significant decrease in SCL (at the conventional 1CDF) and increase in 1CDF (obtained at $1000\ \mathrm{r/min}$) are similar to the theoretical ones, shown in Table IX for faults in phases a and d (c and f). Moreover, the novel PWM method included in the proposed technique avoids overcurrent during transitions, unlike the one used in [7].

Although no more results can be included due to space constraints, it has also been checked that in other fault scenarios the setup behaves as expected from theory. Nevertheless, the most important conclusion from the theory is that the proposed postfault method yields much better performance than the conventional one for a given fault situation, and this has been directly proved with the presented results (see Table XVI).

VI. Conclusion

In this article, a fault-tolerant strategy for two-level asymmetrical six-phase induction motor drives under one or more open- or closed-circuit IGBT faults is proposed. This strategy mainly consists of three novel proposals.

1) Some of the phases with IGBT faults alternate between two modes: keeping the phase open or fixed to the dc-link midpoint O. Although previous postfault strategies rely on keeping the faulty phases open (in two-level multiphase drives) and some others on fixing one to O (in two-level three-phase drives), conveniently switching between these operation modes in a single two-level drive has not been addressed before.
2) It is also proposed to adequately turn ON/OFF a bidirectional switch between the stator neutral points, to further enhance the performance.
3) Moreover, a PWM procedure is proposed to ensure a smooth transition between drive configurations. Overcurrent is avoided by injecting a zero-sequence voltage such that the voltage drop across a bidirectional switch (e.g., a triac or relay) is canceled before it is closed.

The following general guidelines (with a few exceptions, discussed in the article) were defined to set the optimum drive configuration at each moment.

1) For 1N, one phase under fault is fixed to O when $\omega < \omega^{\mathrm{rc}}/2$; and when $\omega > \omega^{\mathrm{rc}}/2$, it is opened.
2) For 2N, one phase under fault is fixed to O per each star when $\omega < \omega^{\mathrm{rc}}/2$; and when $\omega > \omega^{\mathrm{rc}}/2$, it is opened.
3) For SN (preferred), the 2 *N* method is applied if $\omega < \omega^{\mathrm{rc}}/2$; and if $\omega > \omega^{\mathrm{rc}}/2$, 1N is set and all faulty phases are opened.

By applying these principles, on the one hand, the 1CDF (or equivalently, the maximum achievable torque) is increased (e.g., from 55.7% to 100%) and the SCL-per-torque is decreased (e.g., to less than half) in comparison with the usual two-level multiphase approach of keeping all faulty phases open. On the other hand, the maximum speed is raised (and often the 1CDF and SCL-per-torque also improved, by fixing to O two faulty phases) with respect to the existing strategy (applied in two-level three-phase drives) based on permanently fixing to O a single faulty phase. Therefore, since both the maximum torque and maximum speed become larger compared with conventional postfault methods, it can be concluded that, besides reducing the SCL-per-torque, the torque–speed region is extended. In addition, the proposed PWM technique (unlike conventional ones) included in the postfault strategy permits to alter in this manner the drive configuration without overcurrent during transitions.

The price to pay for these benefits is mainly the need for extra fuses and bidirectional switches, as well as a particular converter design with accessible dc-link midpoint and special measures (e.g., oversized capacitors) to avoid oscillations in its voltage. Nevertheless, these shortcomings are often considered acceptable for improving postfault performance in actual motor drives [20], [24], [32].

The theory has been verified by experimental tests.

References

[1] W. N. W. A. Munim, M. J. Duran, H. S. Che, M. Bermúdez, I. González-Prieto, and N. A. Rahim, “A unified analysis of the fault tolerance capability in six-phase induction motor drives,” *IEEE Trans. Power Electron.*, vol. 32, no. 10, pp. 7824–7836, Oct. 2017.

[2] E. Levi, R. Bojoi, F. Profumo, H. A. Toliyat, and S. Williamson, “Multiphase induction motor drives—A technology status review,” *IET Electr. Power Appl.*, vol. 1, no. 4, pp. 489–516, Jul. 2007.

[3] M. Duran and F. Barrero, “Recent advances in the design, modeling and control of multiphase machines—Part 2,” *IEEE Trans. Ind. Electron.*, vol. 63, no. 1, pp. 459–468, Jan. 2016.

[4] H. S. Che, M. J. Duran, E. Levi, M. Jones, W.-P. Hew, and N. Abd Rahim, “Postfault operation of an asymmetrical six-phase induction machine with single and two isolated neutral points,” *IEEE Trans. Power Electron.*, vol. 29, no. 10, pp. 5406–5416, Oct. 2014.

[5] A. S. Abdel-Khalik, A. M. Massoud, and S. Ahmed, “Effect of dc-link voltage limitation on postfault steady-state performance of asymmetrical six-phase induction machines,” *IEEE Trans. Ind. Electron.*, vol. 65, no. 9, pp. 6890–6900, Sep. 2018.

[6] F. Baneira, J. Doval-Gandoy, A. G. Yepes, O. López, and D. Pérez-Estévez, “Control strategy for multiphase drives with minimum losses in the full torque operation range under single open-phase fault,” *IEEE Trans. Power Electron.*, vol. 32, no. 8, pp. 6275–6285, Aug. 2017.

[7] A. G. Yepes, J. Doval-Gandoy, F. Baneira, and H. Toliyat, “Control strategy for dual three-phase machines with two open phases providing minimum loss in the full torque operation range,” *IEEE Trans. Power Electron.*, vol. 33, no. 12, pp. 10044–10050, Dec. 2018.

[8] F. Baneira, J. Doval-Gandoy, A. G. Yepes, O. López, and D. Pérez-Estévez, “Comparison of postfault strategies for current reference generation for dual three-phase machines in terms of converter losses,” *IEEE Trans. Power Electron.*, vol. 32, no. 11, pp. 8243–8246, Nov. 2017.

[9] H. M. Eldeeb, A. S. Abdel-Khalik, and C. M. Hackl, “Postfault full torque-speed exploitation of dual three-phase IPMSM drives,” *IEEE Trans. Ind. Electron.*, vol. 66, no. 9, pp. 6746–6756, Sep. 2019.

[10] H. S. Che, E. Levi, M. Jones, W.-P. Hew, and N. A. Rahim, “Current control methods for an asymmetrical six-phase induction motor drive,” *IEEE Trans. Power Electron.*, vol. 29, no. 1, pp. 407–417, Jan. 2014.

[11] H. S. Che, A. S. Abdel-Khalik, O. Dordevic, and E. Levi, “Parameter estimation of asymmetrical six-phase induction machines using modified standard tests,” *IEEE Trans. Ind. Electron.*, vol. 64, no. 8, pp. 6075–6085, Aug. 2017.

[12] A. G. Yepes, J. Doval-Gandoy, F. Baneira, D. Pérez-Estévez, and O. López, “Current harmonic compensation for n-phase machines with asymmetrical winding arrangement and different neutral configurations,” *IEEE Trans. Ind. Appl.*, vol. 53, no. 6, pp. 5426–5439, Nov. 2017.

[13] A. G. Yepes, J. Doval-Gandoy, and H. Toliyat, “Improvement of postfault performance of multiphase drives in terms of operating region and stator copper loss,” in *Proc. Annu. Conf. IEEE Ind. Electron. Soc.*, Oct. 2018, pp. 5819–5824.

[14] R. Bojoi, A. Tenconi, F. Profumo, G. Griva, and D. Martinello, “Complete analysis and comparative study of digital modulation techniques for dual three-phase ac motor drives,” in *Proc. IEEE 33rd Annu. IEEE Power Electron. Specialists Conf.*, Jun. 2002, vol. 2, pp. 851–857.

[15] M. J. Duran, I. Gonzalez-Prieto, N. Rios-Garcia, and F. Barrero, “A simple, fast, and robust open-phase fault detection technique for six-phase induction motor drives,” *IEEE Trans. Power Electron.*, vol. 33, no. 1, pp. 547–557, Jan. 2018.

[16] X. Wang, Z. Wang, Z. Xu, M. Cheng, W. Wang, and Y. Hu, “Comprehensive diagnosis and tolerance strategies for electrical faults and sensor faults in dual three-phase PMSM drives,” *IEEE Trans. Power Electron.*, vol. 34, no. 7, pp. 6669–6684, Jul. 2019.

[17] X. Wang, Z. Wang, M. Cheng, and Y. Hu, “Remedial strategies of T-NPC three-level asymmetric six-phase PMSM drives based on SVM-DTC,” *IEEE Trans. Ind. Electron.*, vol. 64, no. 9, pp. 6841–6853, Sep. 2017.

[18] Z. Wang, X. Wang, M. Cheng, and Y. Hu, “Comprehensive investigation on remedial operation of switch faults for dual three-phase PMSM drives fed by T-3 L inverters,” *IEEE Trans. Ind. Electron.*, vol. 65, no. 6, pp. 4574–4587, Jun. 2018.

[19] X. Wang, Z. Wang, Z. Xu, J. He, and W. Zhao, “Diagnosis and tolerance of common electrical faults in T-type three-level inverters fed dual three-phase PMSM drives,” *IEEE Trans. Power Electron.*, vol. 35, no. 2, pp. 1753–1769, Feb. 2020.

[20] W. Cao, B. C. Mecrow, G. J. Atkinson, J. W. Bennett, and D. J. Atkinson, "Overview of electric motor technologies used for more electric aircraft (MEA)," *IEEE Trans. Ind. Electron.*, vol. 59, no. 9, pp. 3523–3531, Sep. 2012.

[21] H. Chen, G. Han, X. Shi, and J. Dong, "Phase current digital analysis of power converter for freewheeling diode fault diagnosis on switched reluctance motor drive," *IEEE Trans. Ind. Electron.*, vol. 66, no. 8, pp. 6613–6624, Aug. 2019.

[22] Z. Liu, Z. Zheng, S. D. Sudhoff, C. Gu, and Y. Li, "Reduction of common-mode voltage in multiphase two-level inverters using SPWM with phase-shifted carriers," *IEEE Trans. Power Electron.*, vol. 31, no. 9, pp. 6631–6645, Sep. 2016.

[23] K. Chen and M. Hsieh, "Generalized minimum common-mode voltage PWM for two-level multiphase VSIs considering reference order," *IEEE Trans. Power Electron.*, vol. 32, no. 8, pp. 6493–6509, Aug. 2017.

[24] W. Zhang, D. Xu, P. N. Enjeti, H. Li, J. T. Hawke, and H. S. Krishnamoorthy, "Survey on fault-tolerant techniques for power electronic converters," *IEEE Trans. Power Electron.*, vol. 29, no. 12, pp. 6319–6331, Dec. 2014.

[25] A. S. Abdel-Khalik, M. S. Hamad, A. M. Massoud, and S. Ahmed, "Post-fault operation of a nine-phase six-terminal induction machine under single open-line fault," *IEEE Trans. Ind. Electron.*, vol. 65, no. 2, pp. 1084–1096, Feb. 2018.

[26] A. G. Yepes, J. Doval-Gandoy, F. Baneira, and H. Toliyat, "Comparison of stator winding connections in multiphase drives under healthy operation and with one open converter leg," *ET Elect. Power Appl.*, vol. 14, no. 4, pp. 584–596, Apr. 2020.

[27] H.-M. Ryu, J.-W. Kim, and S.-K. Sul, "Synchronous-frame current control of multiphase synchronous motor under asymmetric fault condition due to open phases," *IEEE Trans. Ind. Appl.*, vol. 42, no. 4, pp. 1062–1070, Jul./Aug. 2006.

[28] A. Tani, M. Mengoni, L. Zarri, G. Serra, and D. Casadei, "Control of multiphase induction motors with an odd number of phases under open-circuit phase faults," *IEEE Trans. Power Electron.*, vol. 27, no. 2, pp. 565–577, Feb. 2012.

[29] L. Cheng, Y. Sui, P. Zheng, P. Wang, and F. Wu, "Implementation of postfault decoupling vector control and mitigation of current ripple for five-phase fault-tolerant PM machine under single-phase open-circuit fault," *IEEE Trans. Power Electron.*, vol. 33, no. 10, pp. 8623–8636, Oct. 2018.

[30] M. Tousizadeh, H. S. Che, J. Selvaraj, N. A. Rahim, and B. Ooi, "Performance comparison of fault-tolerant three-phase induction motor drives considering current and voltage limits," *IEEE Trans. Ind. Electron.*, vol. 66, no. 4, pp. 2639–2648, Apr. 2019.

[31] M. Tousizadeh, H. S. Che, J. Selvaraj, N. A. Rahim, and B. Ooi, "Fault-tolerant field-oriented control of three-phase induction motor based on unified feedforward method," *IEEE Trans. Power Electron.*, vol. 34, no. 8, pp. 7172–7183, Aug. 2019.

[32] B. A. Welchko, T. A. Lipo, T. M. Jahns, and S. E. Schulz, "Fault tolerant three-phase ac motor drive topologies: a comparison of features, cost, and limitations," *IEEE Trans. Power Electron.*, vol. 19, no. 4, pp. 1108–1116, Jul. 2004.

[33] E. Levi, "FOC: Field oriented control," in *The Industrial Electronics Handbook*, vol. Power Electronics and Motor Drives. Boca Raton, FL, USA: CRC Press, 2011.

[34] E. Levi, D. Dujic, M. Jones, and G. Grandi, "Analytical determination of dc-bus utilization limits in multiphase VSI supplied ac drives," *IEEE Trans. Energy Convers.*, vol. 23, no. 2, pp. 433–443, Jun. 2008.

[35] T.-H. Liu, J.-R. Fu, and T. A. Lipo, "A strategy for improving reliability of field-oriented controlled induction motor drives," *IEEE Trans. Ind. Appl.*, vol. 29, no. 5, pp. 910–918, Sep. 1993.

[36] O. López *et al.*, "Carrier-based PWM equivalent to multilevel multiphase space vector PWM techniques," *IEEE Trans. Ind. Electron.*, vol. 67, no. 7, pp. 5220–5231, Jul. 2020.

[37] W. N. W. A. Munim, M. Tousizadeh, and H. S. Che, "Effects of zero-sequence transformations and min-max injection on fault-tolerant symmetrical six-phase drives with single isolated neutral," *J. Power Electron.*, vol. 19, no. 4, pp. 968–979, Jul. 2019.

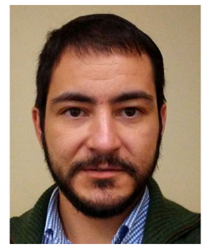

Alejandro G. Yepes (Senior Member, IEEE) received the M.Sc. and Ph.D. degrees in electrical engineering from the University of Vigo, Vigo, Spain, in 2009 and 2011, respectively.

Since 2008, he has been working with the Applied Power Electronics Technology Research Group, University of Vigo. From August 2016 to June 2018, he stayed with the Department of Electrical and Computer Engineering, Texas A&M University, College Station, TX, USA, after which he returned to the University of Vigo. His research interests include the areas of ac power conversion, with special focus, currently, on multiphase drives.

Jesús Doval-Gandoy (Member, IEEE) received the M.Sc. degree from the Polytechnic University of Madrid, Madrid, Spain, in 1991, and the Ph.D. degree from the University of Vigo, Vigo, Spain, in 1999, both in electrical engineering.

He is currently a Professor and the Head of the Applied Power Electronics Technology Research Group (APET), University of Vigo. His research interests include the areas of ac power conversion.

Hamid A. Toliyat (Fellow, IEEE) received the B.S. degree from the Sharif University of Technology, Tehran, Iran, in 1982, the M.S. degree from West Virginia University, Morgantown, WV, USA, in 1986, and the Ph.D. degree from the University of Wisconsin-Madison, Madison, WI, USA, in 1991, all in electrical engineering.

Following receipt of the Ph.D. degree, he joined the Ferdowsi University of Mashhad, Mashhad, Iran, as an Assistant Professor of electrical engineering. In March 1994, he joined the Department of Electrical and Computer Engineering, Texas A&M University, College Station, TX, USA, where he is currently a Raytheon Endowed Professor of electrical engineering.